NATIONAL ENERGY TECHNOLOGY LABORATORY

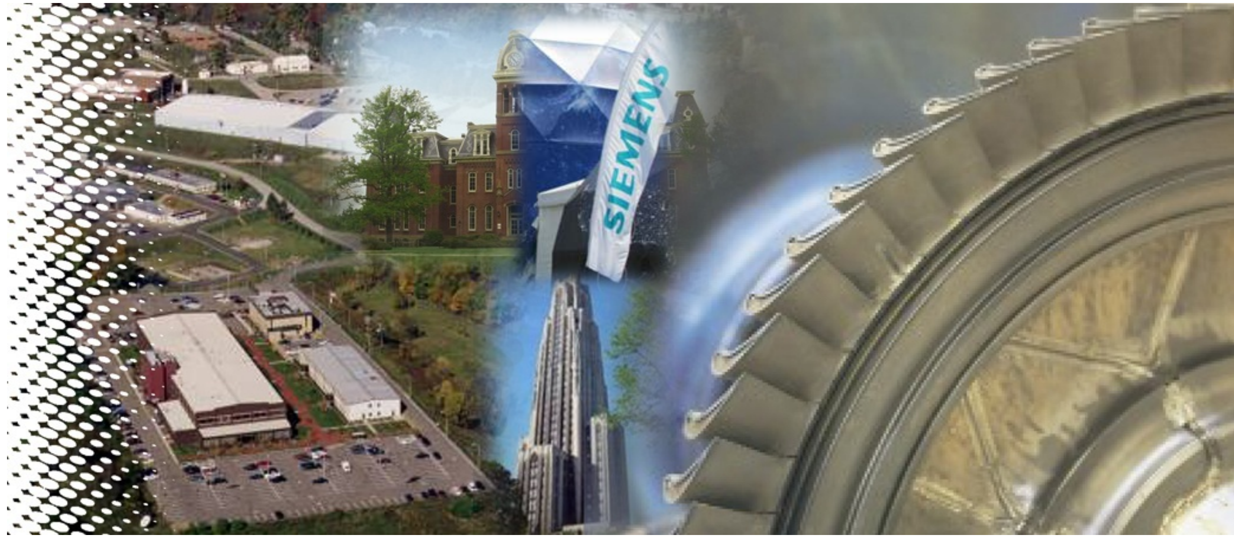

Integrated Transpiration and Lattice Cooling Systems Developed by Additive Manufacturing with Oxide-Dispersion-Strengthened (ODS) Alloys

Minking Chyu, Albert To
University of Pittsburgh

Bruce S. Kang
West Virginia University

Oct 30, 2018

Transpiration Cooling vs Film Cooling

- Film cooling
  - Large hole size
  - Discrete hole pitch

- "Lift-off" of the film due to jet momentum at the outlet
- Film gradually spread diffused downstream by flow mixing

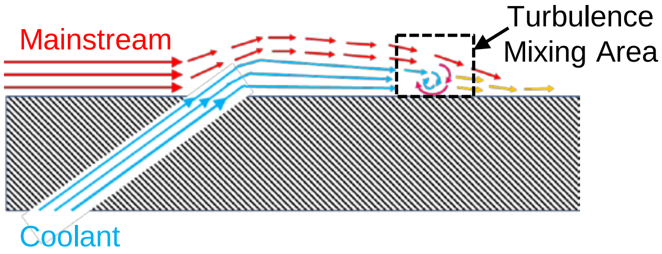

- Transpiration cooling
  - Porous wall or multiple micro-channels
  - Large solid-fluid interface inside the wall
  - Uniform coolant discharge & distribution

- More uniform coolant film coverage
- Coolant convected through pores
- Increased heat removal ability due to higher inter-wall heat transfer

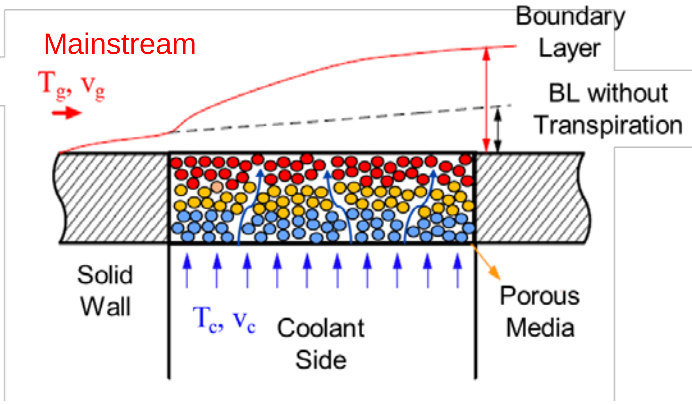

Unit Cells for Lattice Cooling

Overview of unit cells under investigation:

<u>Tetrahedral</u>

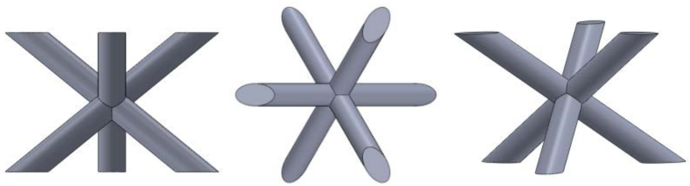

Front View Top view Perspective

<u>Face centered (FC)</u>

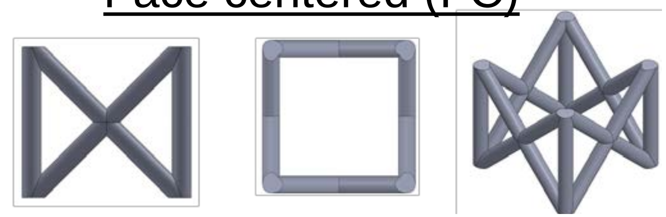

Front View Top view Perspective

<u>Body centered (BC)</u>

Front View Top view Perspective

<u>Octahedral (Octa)</u>

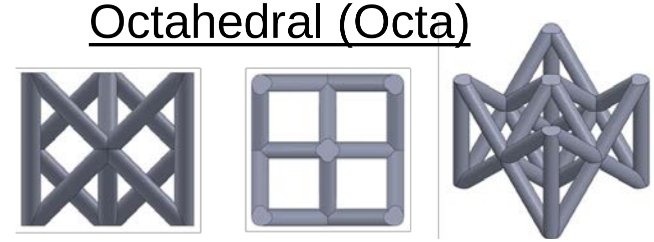

Front View Top view Perspective

Parameters	
Ligament diameter:	d
Unit cell base:	a
Unit cell height:	h
Porosity:	p
Total surface area:	A_{surf}
Footprint area:	A_{fp}
Orientation with flow:	θ

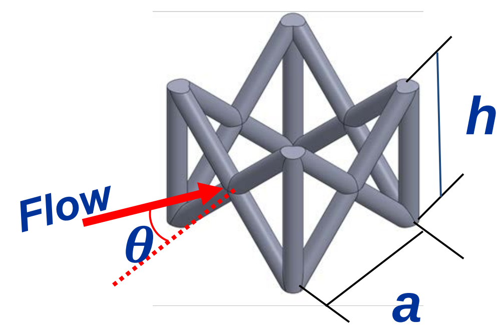

Flow Field

Re based on channel diameter = 15,000

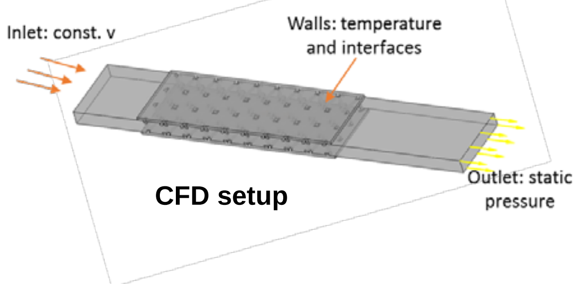

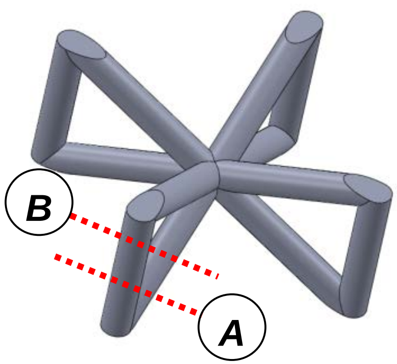

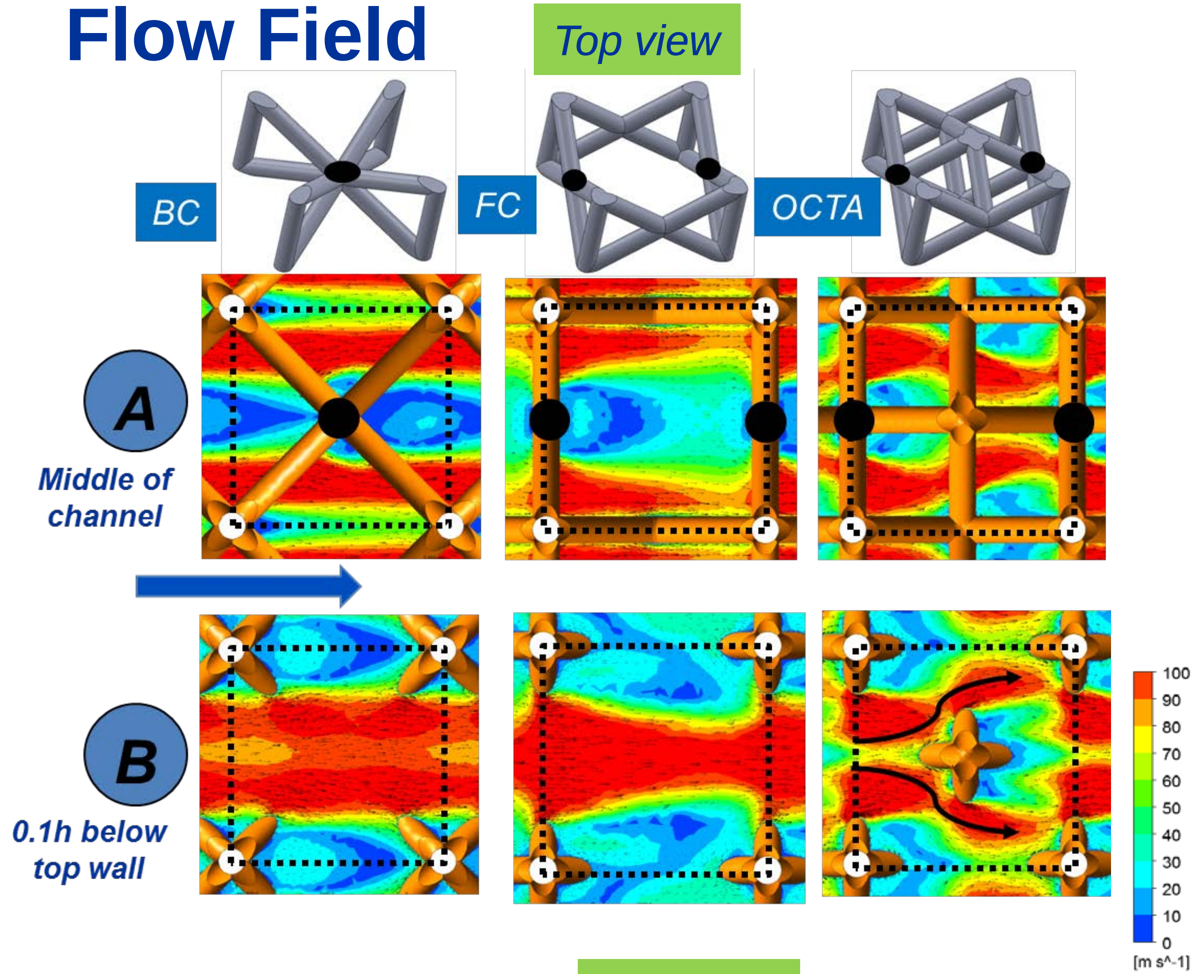

- ➢ Flow field shaped by nodes and openings in unit cell.
- ➢ High speed flow confined in virtual subchannels.

- ➢ Nodes divert and help confine flow closer to end walls.

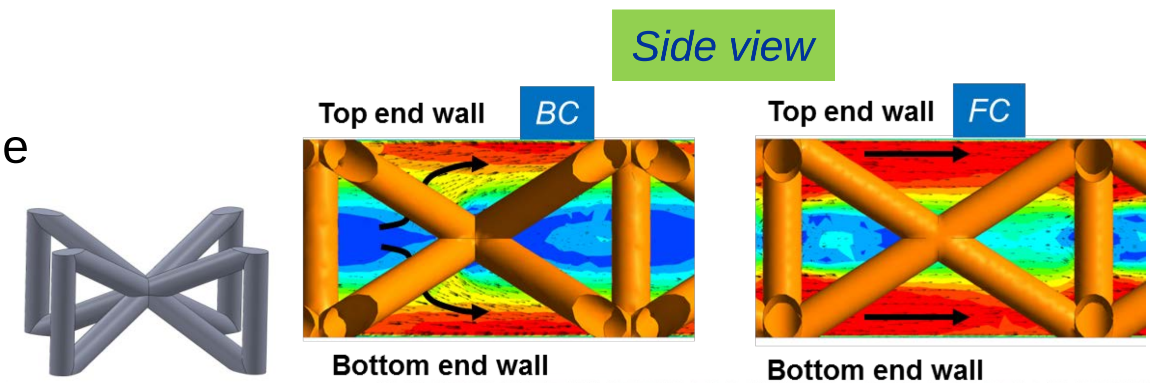

Project Work Breakdown Structure

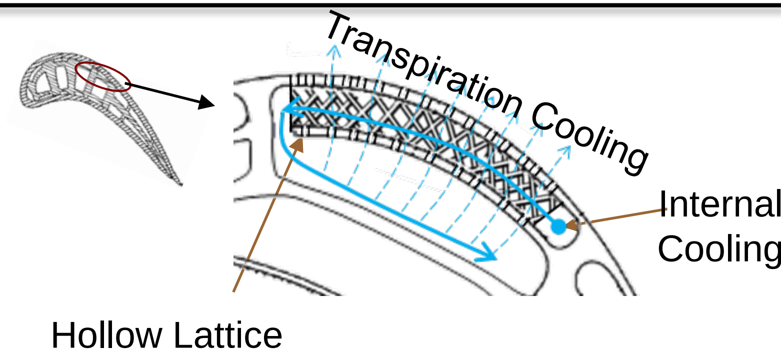

Integrated Transpiration and Lattice Cooling Systems

Enhanced Thermal Protection

- *Lattice and transpiration combined conjugate cooling*
- *~2x of state-of-the-art film cooling.*

Novel Metallic ODS Lattice Structure

- *Ultra-High Temperature (1200℃) Strength*
- *Oxidation Resistance*
- *Realized with additive manufacturing*

Task 2 – Heat Transfer Characterization

- *Design, CFD modeling & scaled testing*
- *Mini/micro scale cellular units*

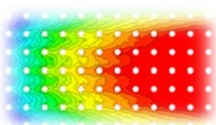

Task 5 – High Temperature Heat Transfer Characterization

High Temperature, Pressurized Testing (NETL)

Task 6 – ODS Powder Fabrication and Characterization

- *ODS powders fabrication*
- *Characterization*

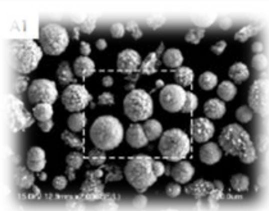

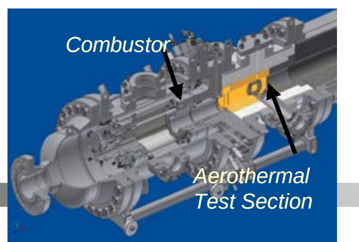

Task 3 – Multi-Objective Topology Optimization

- *Geometry development and optimization*

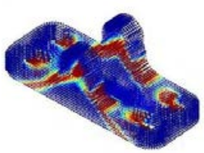

Task 4 – Process Optimization to Fabricate ODS Lattice Structures

- *Printing parameters*
- *Posting printing characterization*
- *OM, SEM,*

Task 7 – Thermal Cyclic Testing

- *In-situ non-destructive micro indentation facility*
- *Thermal Cyclic Tests, Micro-hardness*

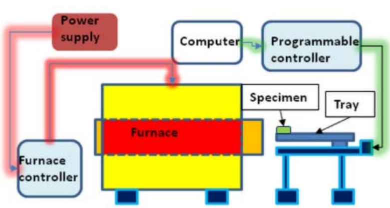

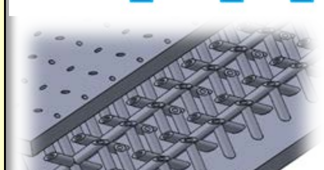

Outlines

- *Introduction and Background*
- *Challenges, Objectives, Benefits of Technology, Research Task Plan*
- *Tasks (Pitt & WVU)*
  1. *Project Management*
  2. *Heat Transfer Characterization*
  3. *Design Optimization*
  4. *Fabrication of ODS Lattice/Transpiration Structures*
  5. *High Temperature Heat Transfer Characterization*
  6. *Production Process for ODS Powder*
  7. *Thermal Cycling Experiments*

Atomization Powder Fabrication Techniques
(Current Standard for Metal AM)

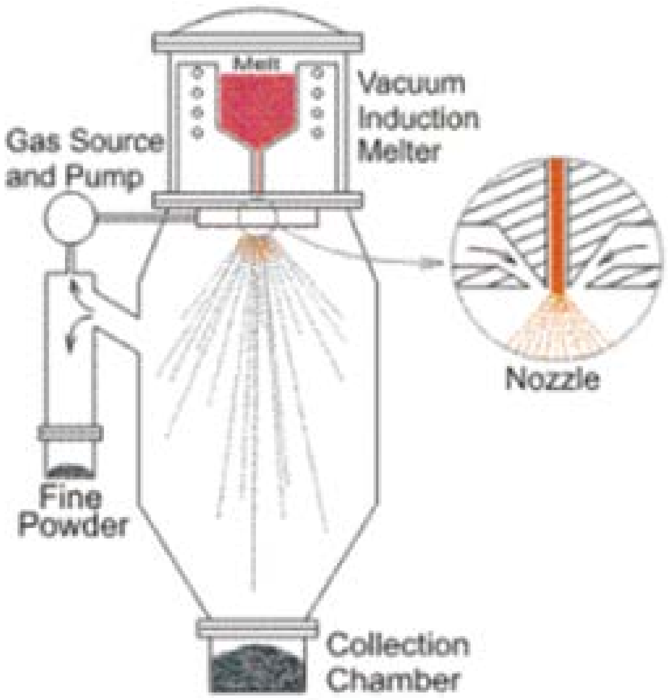

A schematic of Gas Atomization

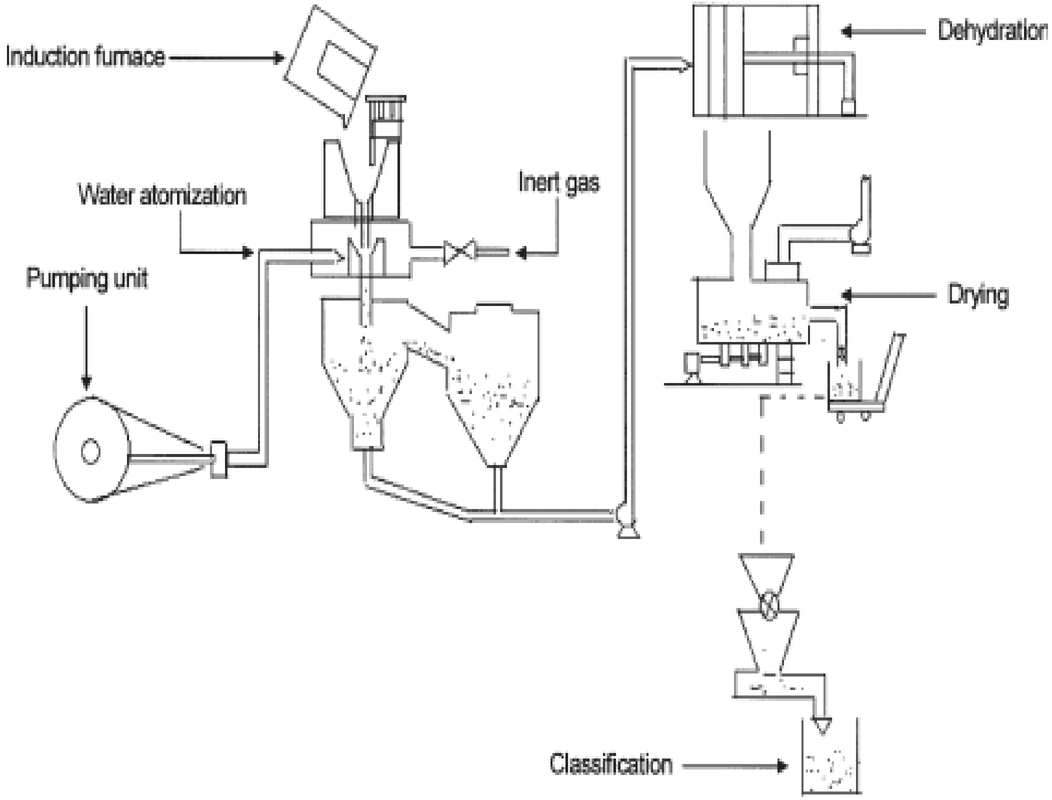

A schematic of Water Atomization

Antony, L. V., & Reddy, R. G. (2003). Processes for production of high-purity metal powders. *Jom*, *55*(3), 14-18.

WestVirginiaUniversity.
BENJAMIN M. STATLER COLLEGE OF ENGINEERING AND MINERAL RESOURCES

Gas Atomization (GA) Metal Powders

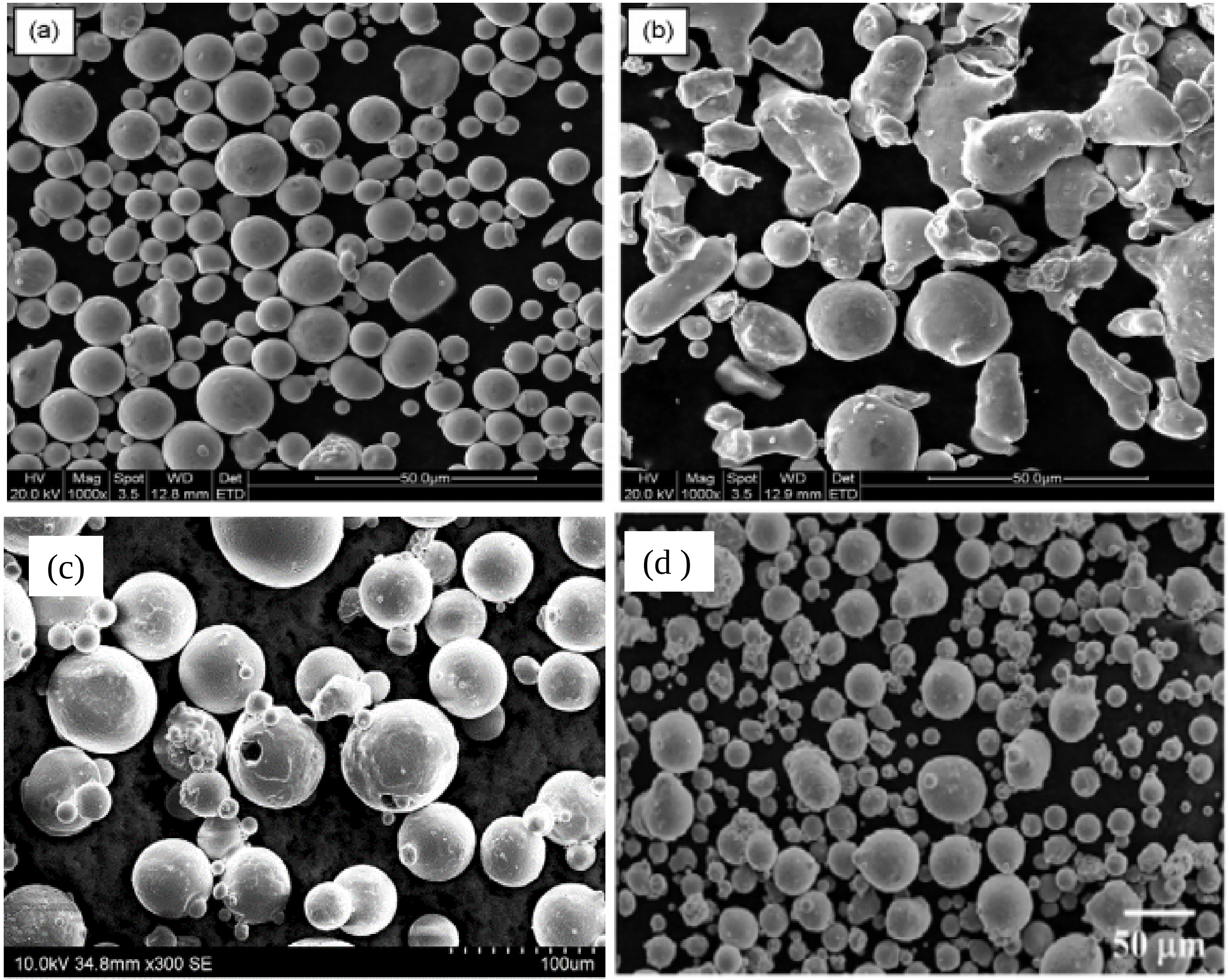

SEM images showing characteristic morphologies of Atomized powder: (a) gas atomized 316 stainless steel; (b) water atomized 316 stainless steel; (c) gas atomized Ti-6Al-4V; (d) gas atomized IN718

Ahsan, M. Naveed, et al. "A comparative study of laser direct metal deposition characteristics using gas and plasma-atomized Ti–6Al–4V powders." *Materials Science and Engineering: A* 528.25-26 (2011): 7648-7657.

Choi, Joon-Phil, et al. "Densification and microstructural investigation of Inconel 718 parts fabricated by selective laser melting." Powder Technology 310 (2017): 60-66.

Li, Ruidi, et al. "Densification behavior of gas and water atomized 316L stainless steel powder during selective laser melting." Applied surface science 256.13 (2010): 4350-4356.

West Virginia University
BENJAMIN M. STATLER COLLEGE OF ENGINEERING AND MINERAL RESOURCES

Principles of MCB

Why MCB?

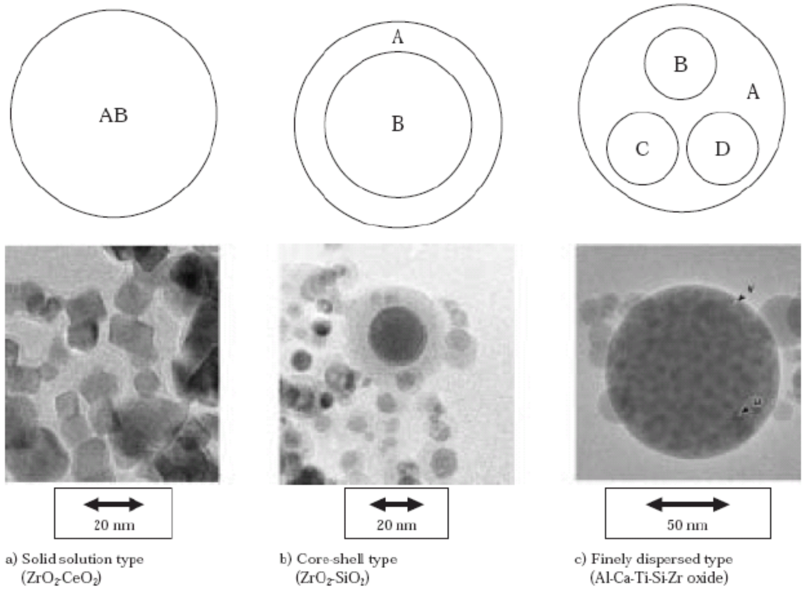

Structural patterns of nanocomposite particles
[T. Yokoyama and C. C. Huang, KONA No.23 (2005)]

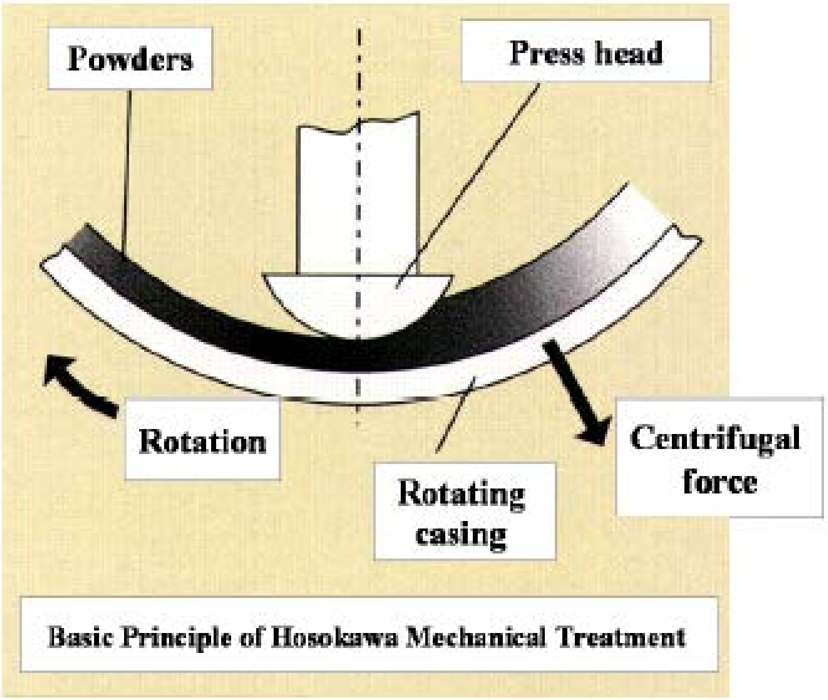

- Capable of fracturing and then uniformly dispersing/bonding nano-sized oxide particles (Y_2O_3) onto base(host) metal particles (< 1 hour processing time).
- Improved particle **sphericity**, ideal for precision mixing of nano and submicron powders.
- Grain boundaries of host particles are pinned by nano-oxide particles (i.e. Y_2O_3), minimized grain growth during sintering

Kang, B.S., Chyu, M.K., Alvin, M.A., and Gleeson, B.M, "Method of Producing an Oxide Dispersion Strengthened Coating and Micro-Channels," US Patent 8609187 B1, 17, 2013

ODS Material System

Elemental ODS Powder			
Elemental powder	**Average Size**	**Degree of purity**	**Weight Percentage**
Nickel	3~7 μm	99.9%	70.5%
Chromium	3~7 μm	99.2%	20%
Aluminum	4.5~7 μm	97.5%	5%
Tungsten	<1 μm	99.95%	3%
Yttrium Oxide	50~70 nm	99.995%	1.5%

MCB+BM

Configuration	Speed(rpm)	BPR	Time(hours)
C1	300	15:1	15
C2	300	30:1	15
C3	300	10:1	25
C4	300	30:1	45
C5	400	15:1	20
C6	400	15:1	40

XRD of ODS Powders MCB only, MCB + Ball Mill for 20 hours, and MCB + Ball Mill for 40 hours.

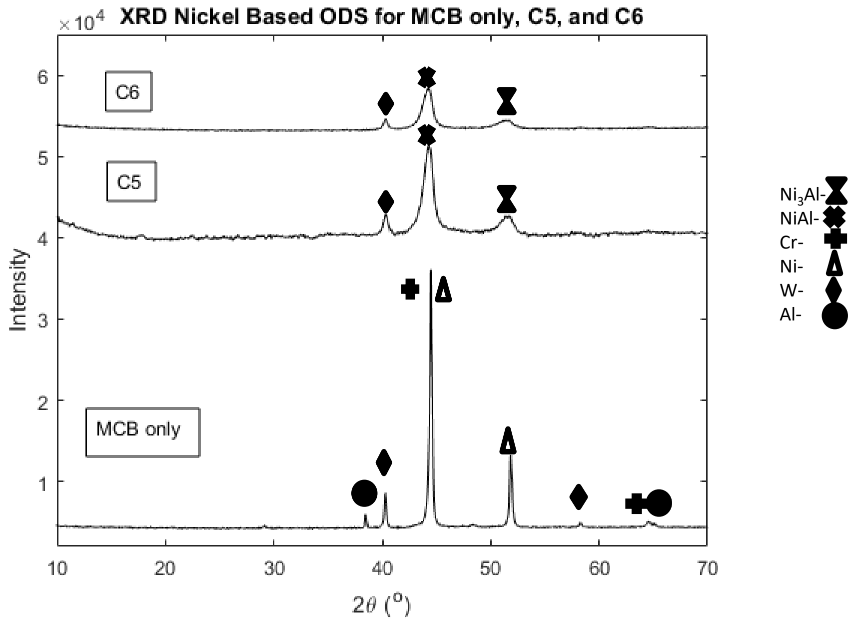

- C5 depicts MCB plus ball milling process for 20 hours at 400 rpm, with a BPR of 15:1.
- C6 depicts MCB plus ball milling process for 40 hours at 400 rpm, with a BPR of 15:1.

ODS Powder Fabrication Optimization (MCB + BM)

BPR: 10, MCB + 25 hours BM

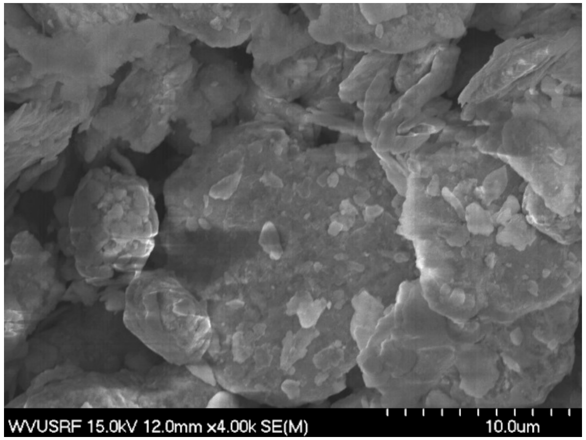

BPR: 15, MCB + 15 hours BM

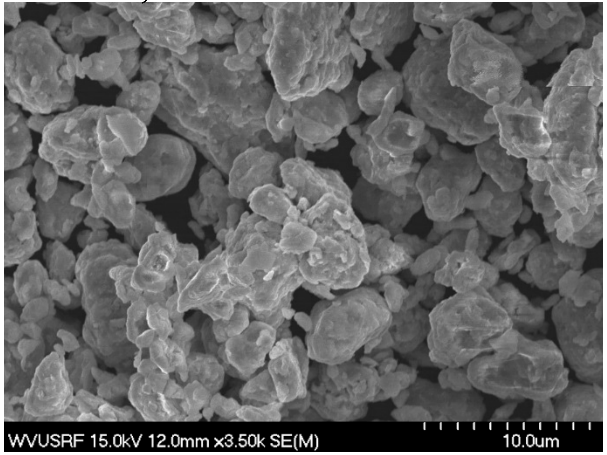

BPR: 30, MCB + 45 hours BM

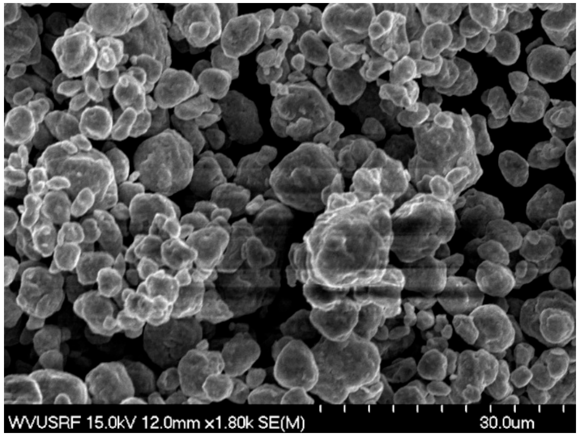

BPR:30, MCB + 15 hours BM

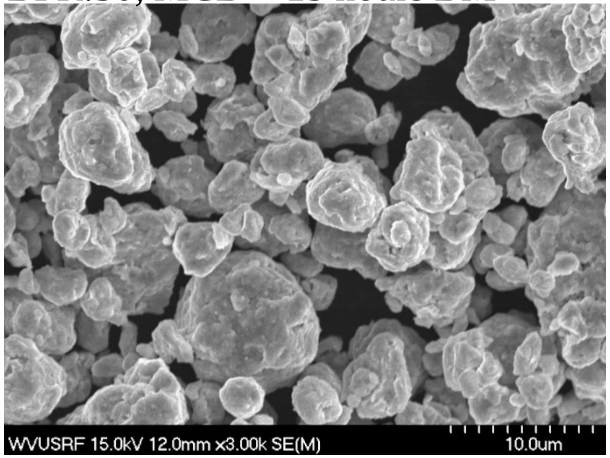

**BPR: Ball to Powder Ratio

WestVirginiaUniversity
BENJAMIN M. STATLER COLLEGE OF
ENGINEERING AND MINERAL RESOURCES

ODS Powder processed by MCB+BM

Ni-20Cr-5Al-3W-1.5Y2O3 in Weight.%

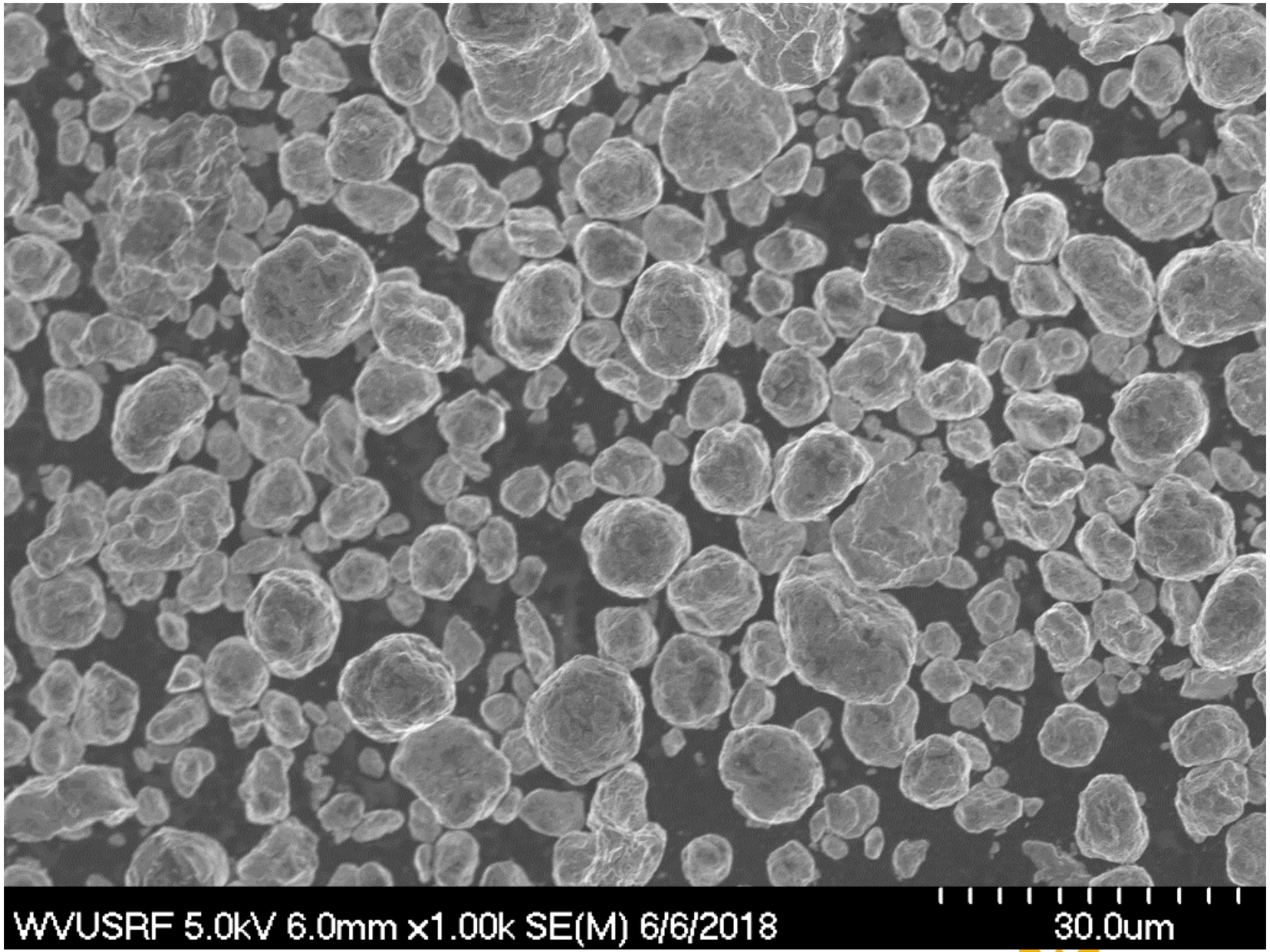

MCB only
(for EOS M290 AM)

MCB-only Processing Parameters			
Configuration	Speed(rpm)	Running Mode	Time(hours)
M1	4000	Normal	1
M2	4000	Normal	18
M3	4000	Normal	32
M4	4000	Normal	50
M5	5000	Normal	32
M6	5000	Normal	50
M7	5000	Step-running	8
M8	5000	Step-running	11

WestVirginiaUniversity
BENJAMIN M. STATLER COLLEGE OF
ENGINEERING AND MINERAL RESOURCES

MCB only 4000 rpm 50hrs (M4)

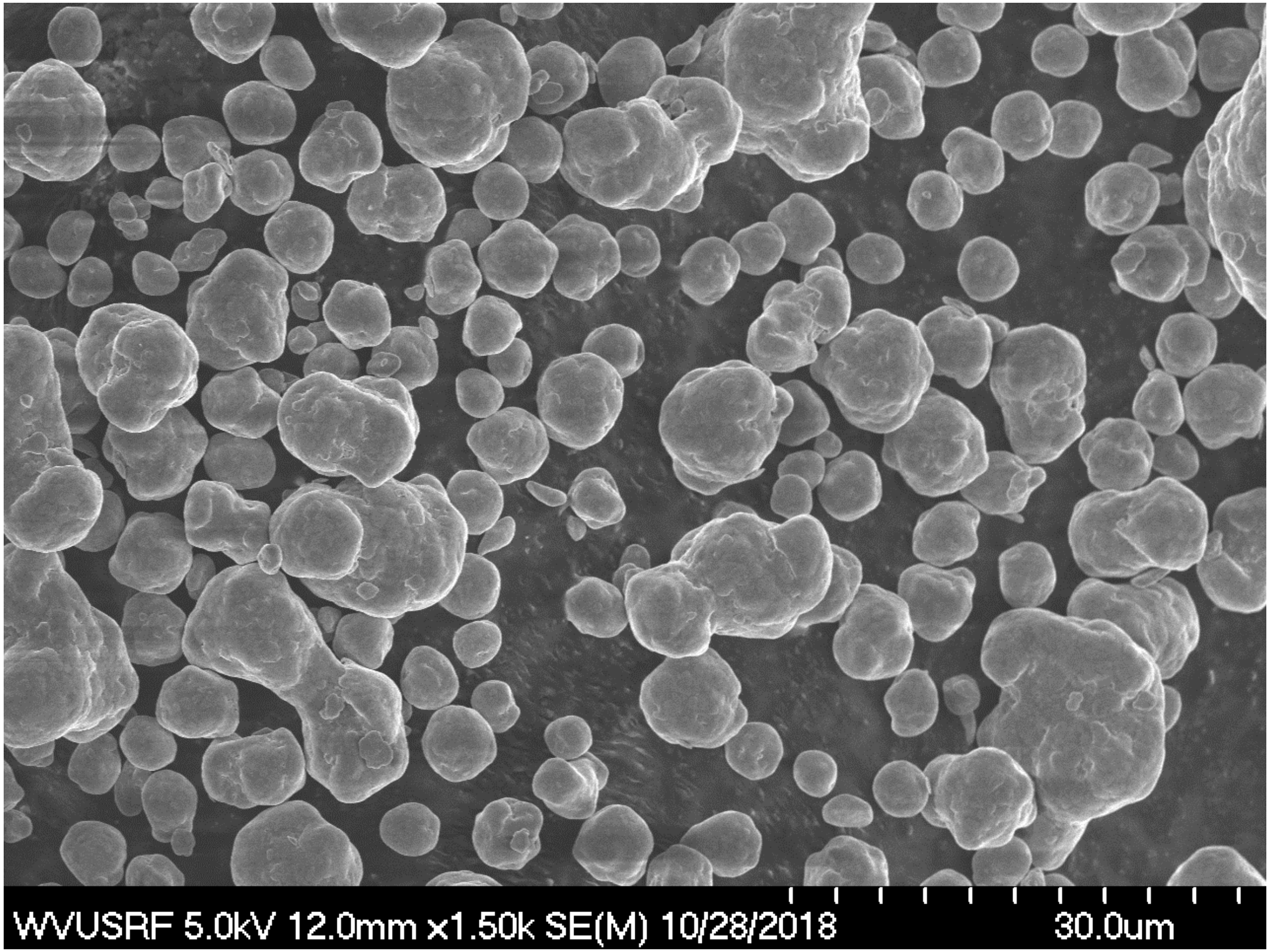

Size Distribution of M6 powders

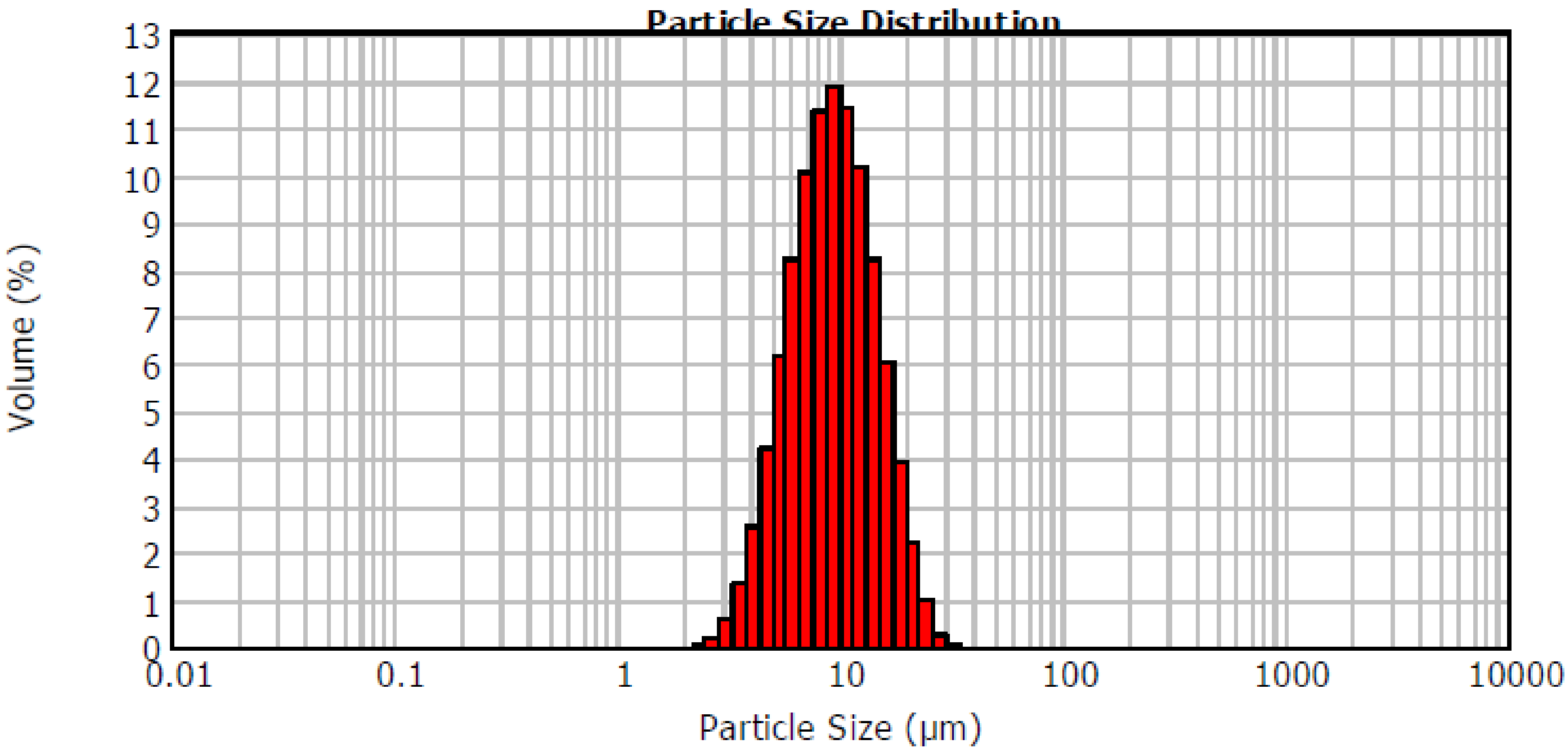

D(0.1)=5.153μm, D(0.5)=9.261μm, D(0.9)=16.296μm

Metallic Additive Manufacturing

Bind Jetting

Pros: geometry free
cons: high porosity

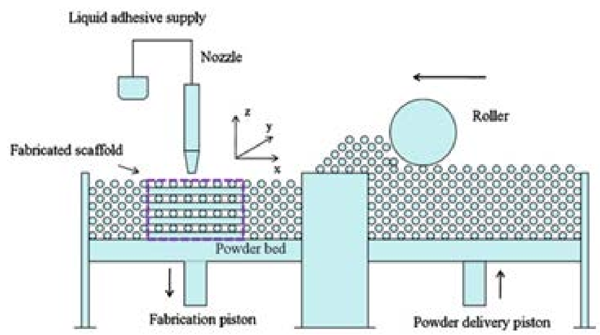

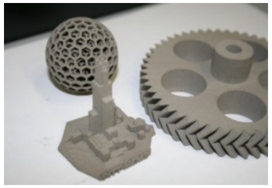

Powder Bed Fusion

Pros: complex geometry
cons: single material

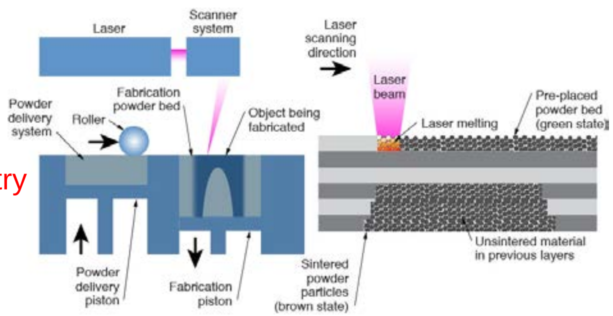

Direct Energy Deposition

Pros: multiple materials
cons: no overhangs or unsupported structure

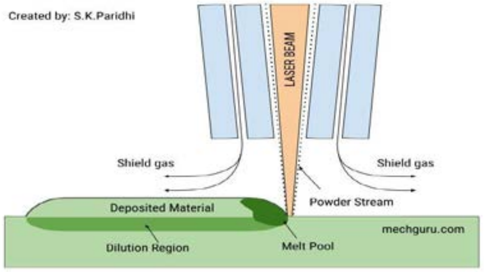

As metallic additive manufacturing technologies matured, it became possible for complex metal product to be manufactured by this innovative technology, which also provides great capabilities to make complex geometries for turbine airfoil cooling channels.

LENS (AM-Printed) ODS Coating on M247 Substrate Coupon

200W Laser Power Coating

150W Laser Power Coating

100W Laser Power Coating

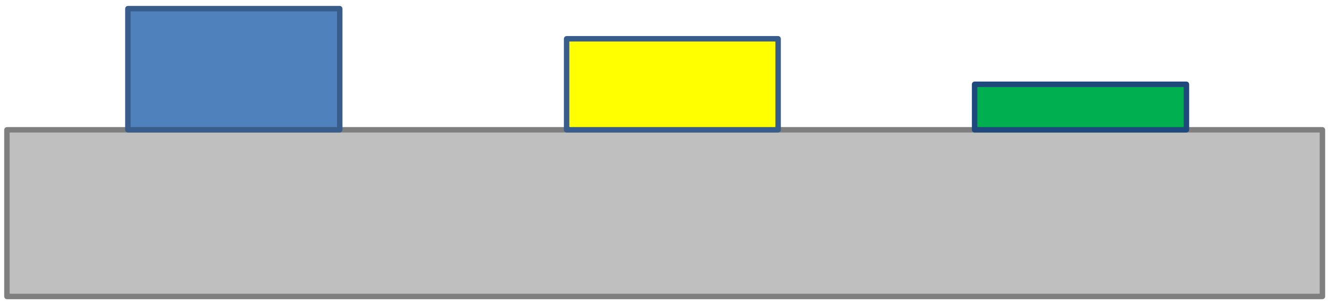

Microstructures of 200W LENS ODS Coating

200W As-printed ODS Coating

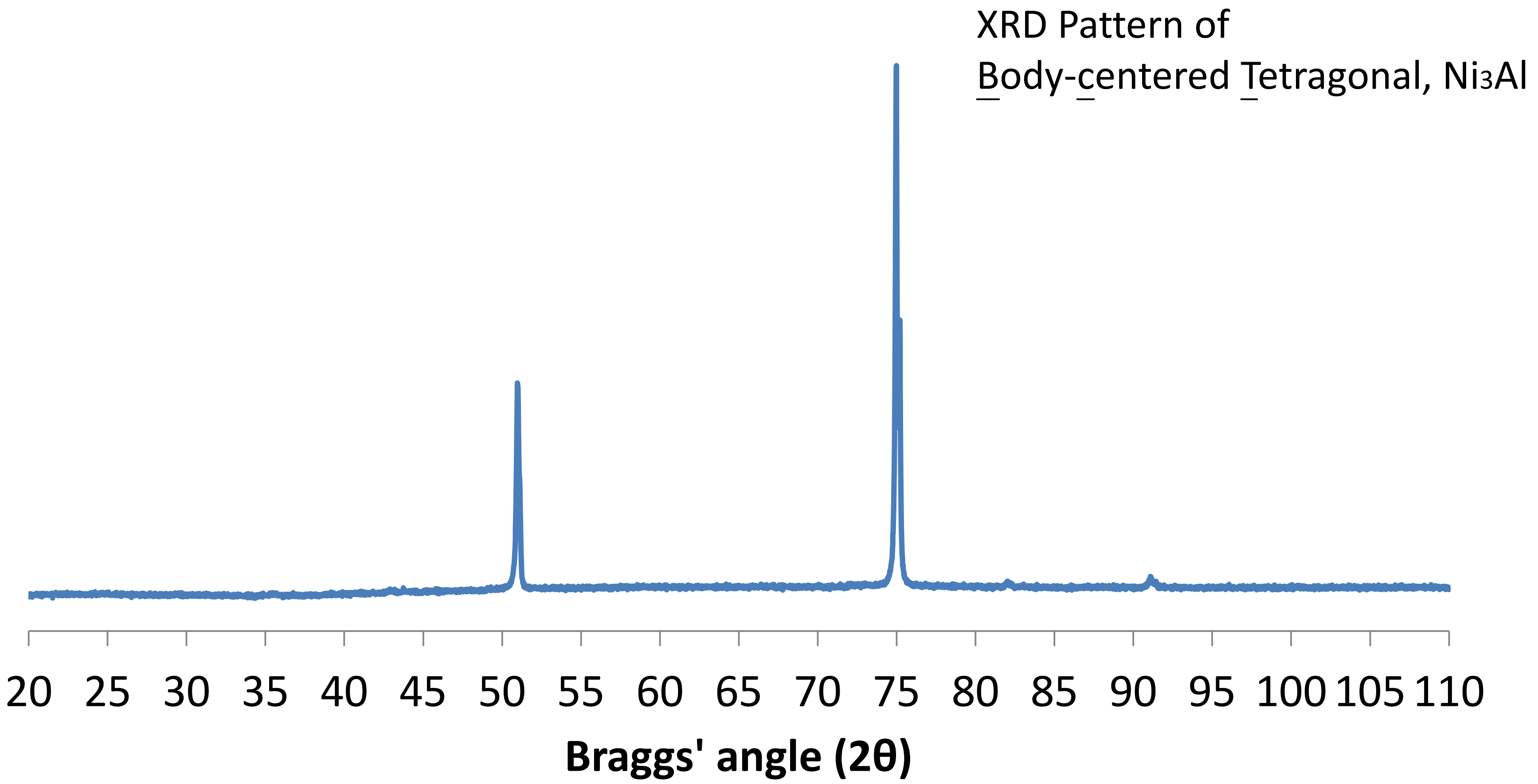

XRD of 200W ODS Coating after 2200 thermal cycles

- Slowly stabilized to form FCC γ-matrix and γ’phase throughout thermal cycles

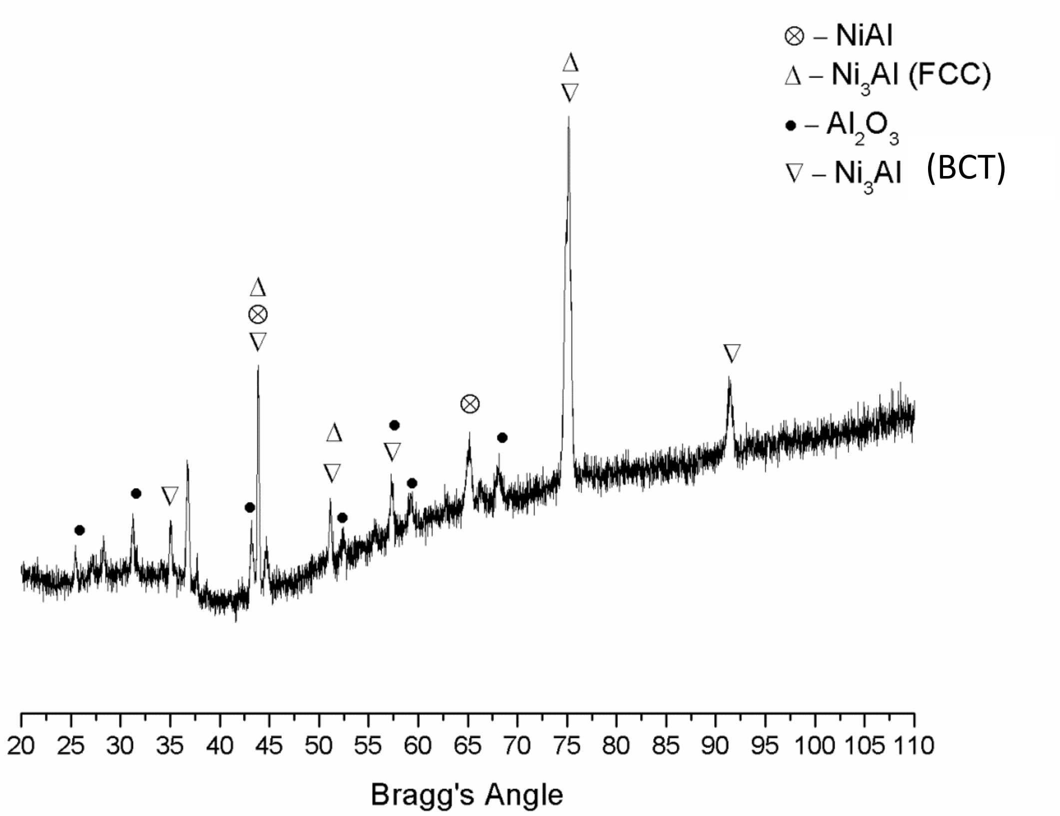

γ′ phase in 200W ODS Coating (DED AM)

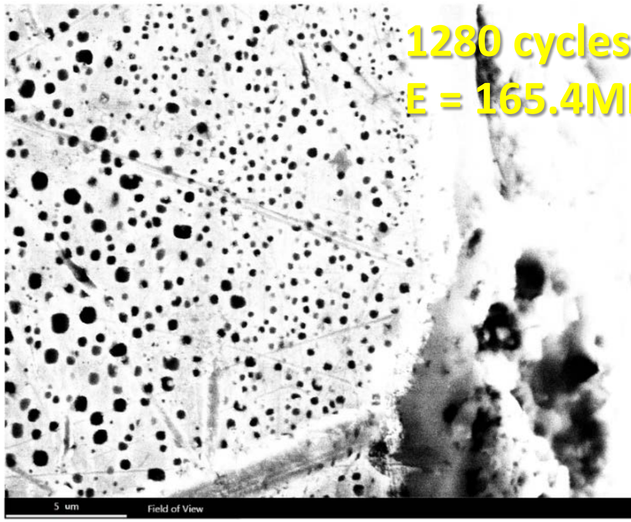

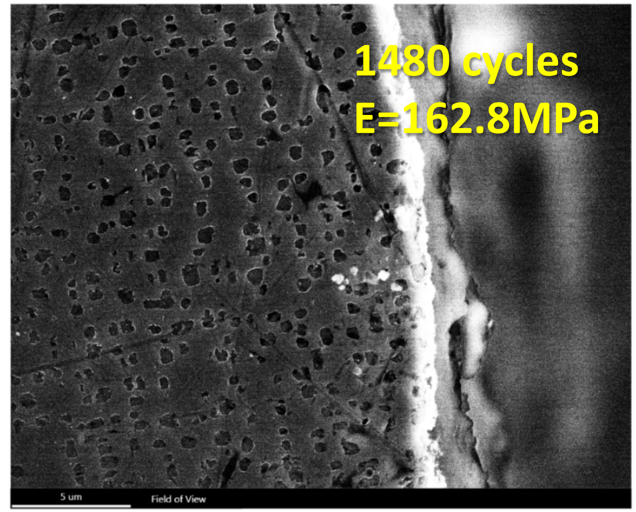

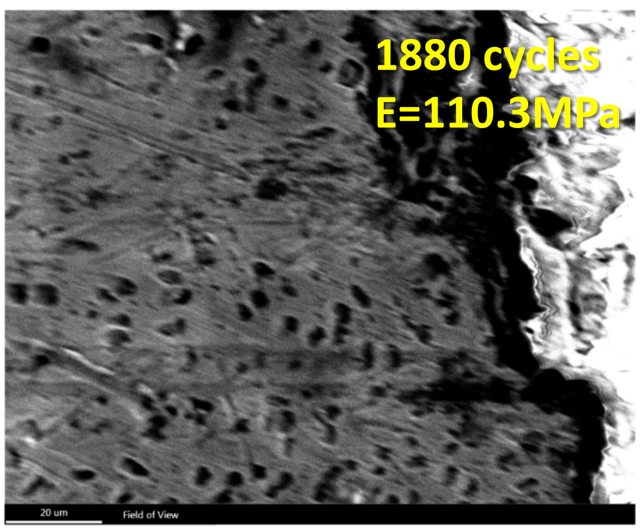

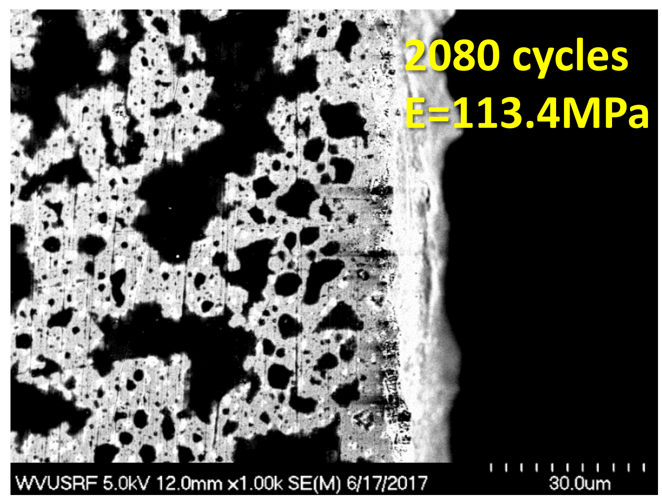

200W ODS – AM Printed

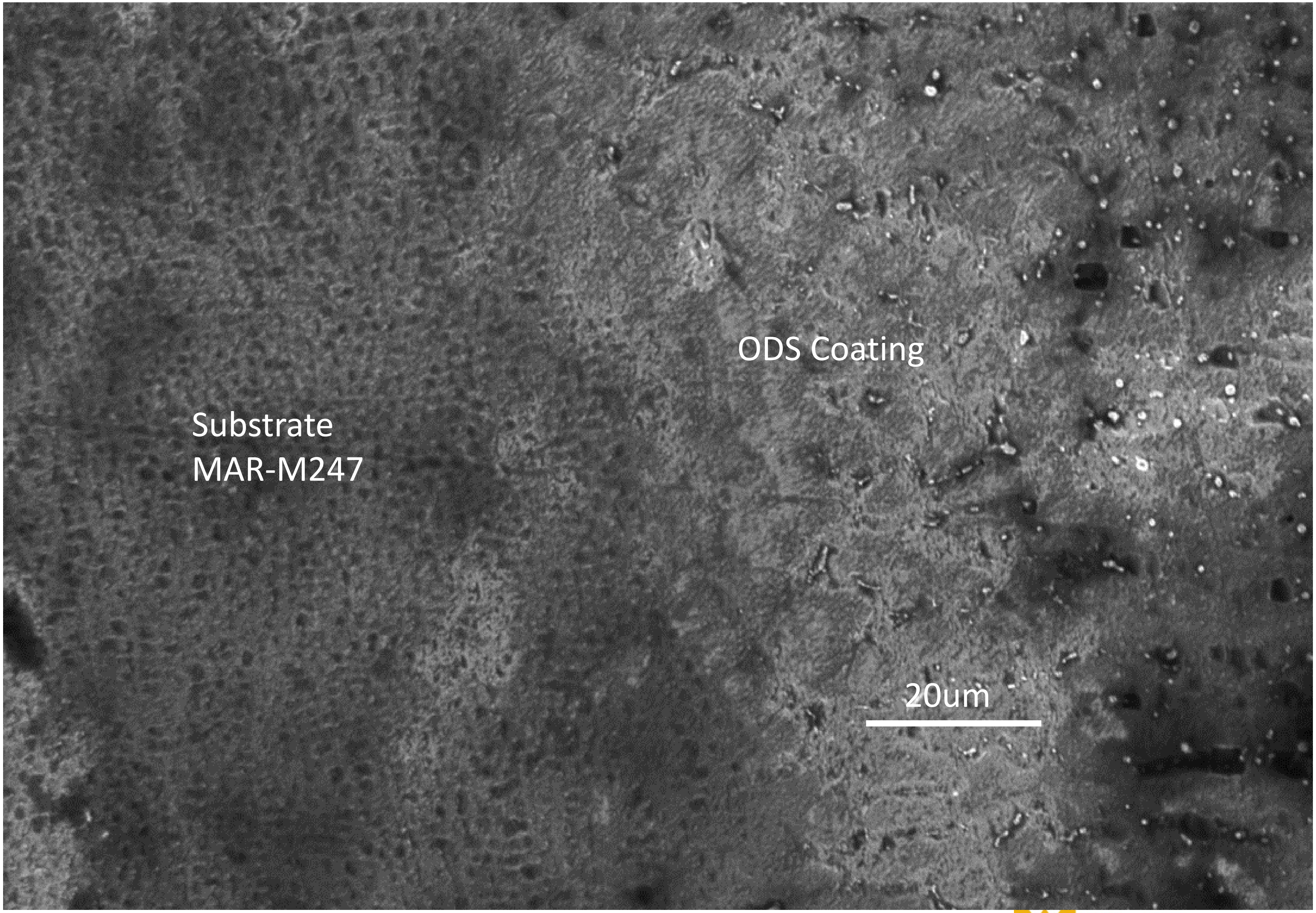

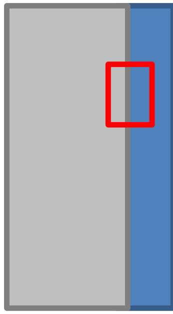

Interface

200W ODS – AM Printed

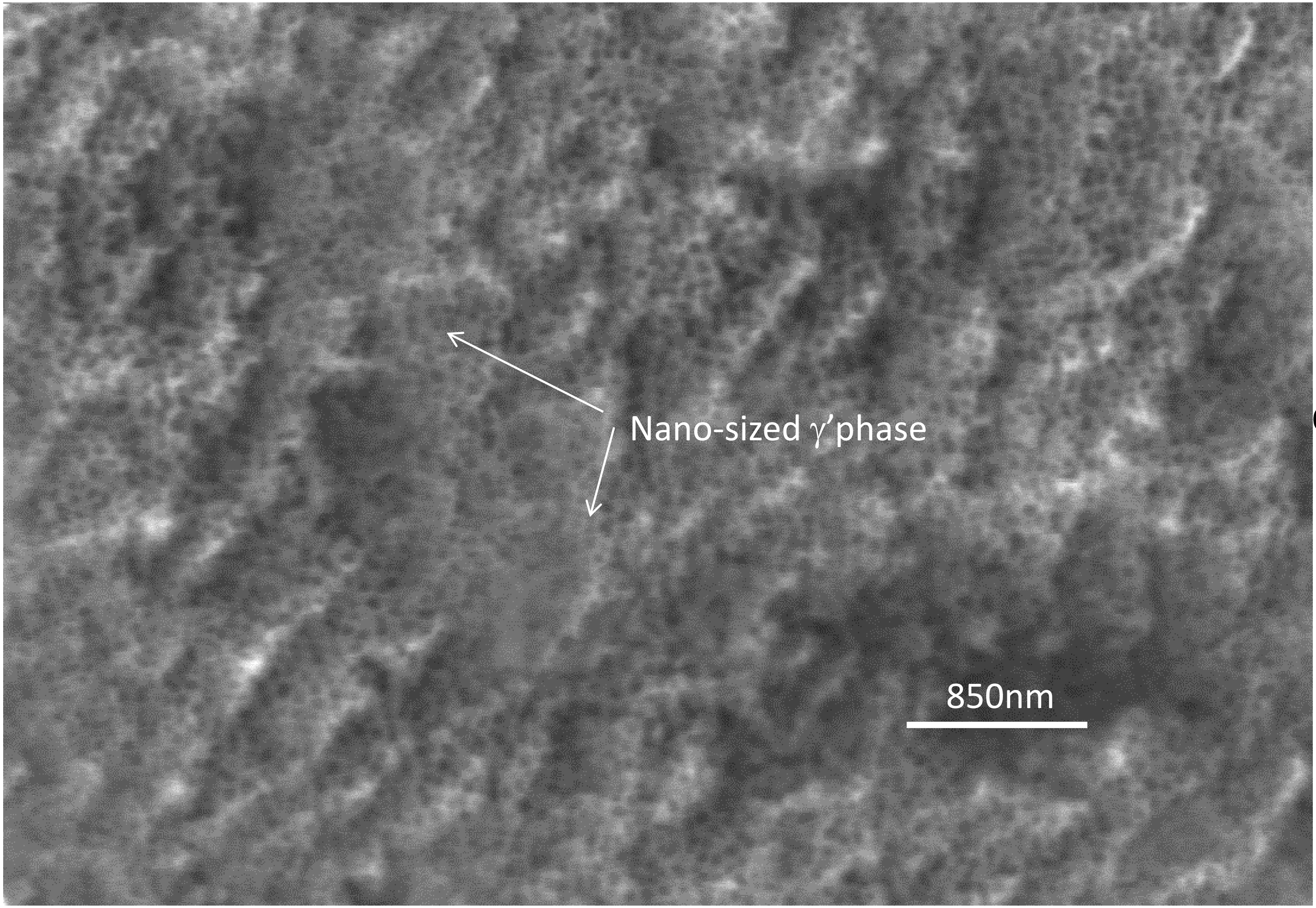

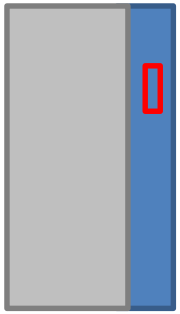

ODS Coating

200W ODS – 2200 Cycles

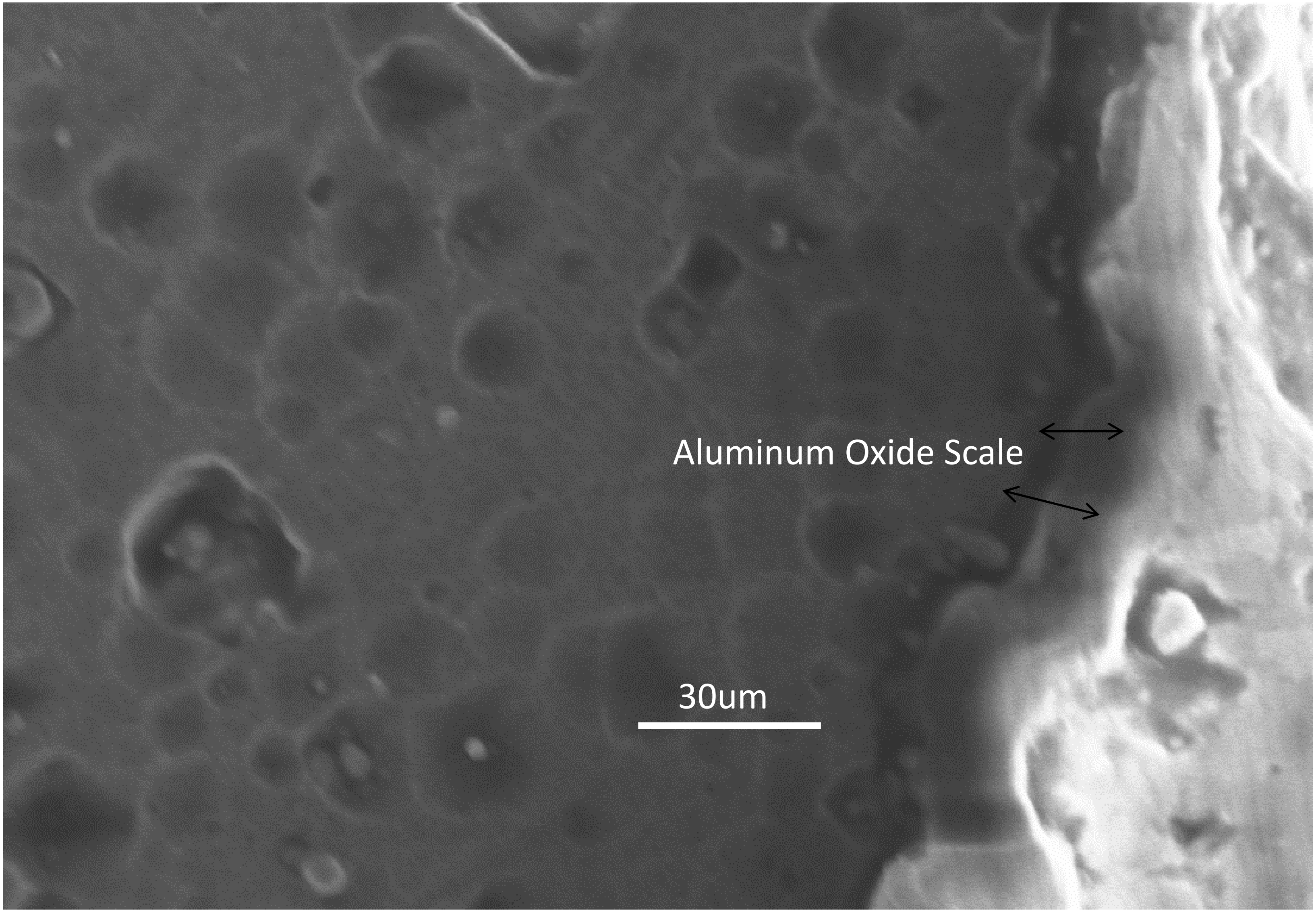

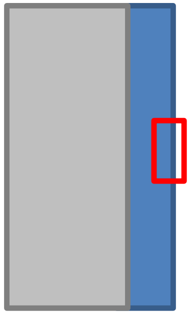

Stable 10 – 15 um of uniform stable aluminum oxide scale

West Virginia University
BENJAMIN M. STATLER COLLEGE OF ENGINEERING AND MINERAL RESOURCES

200W ODS – 2200cycles

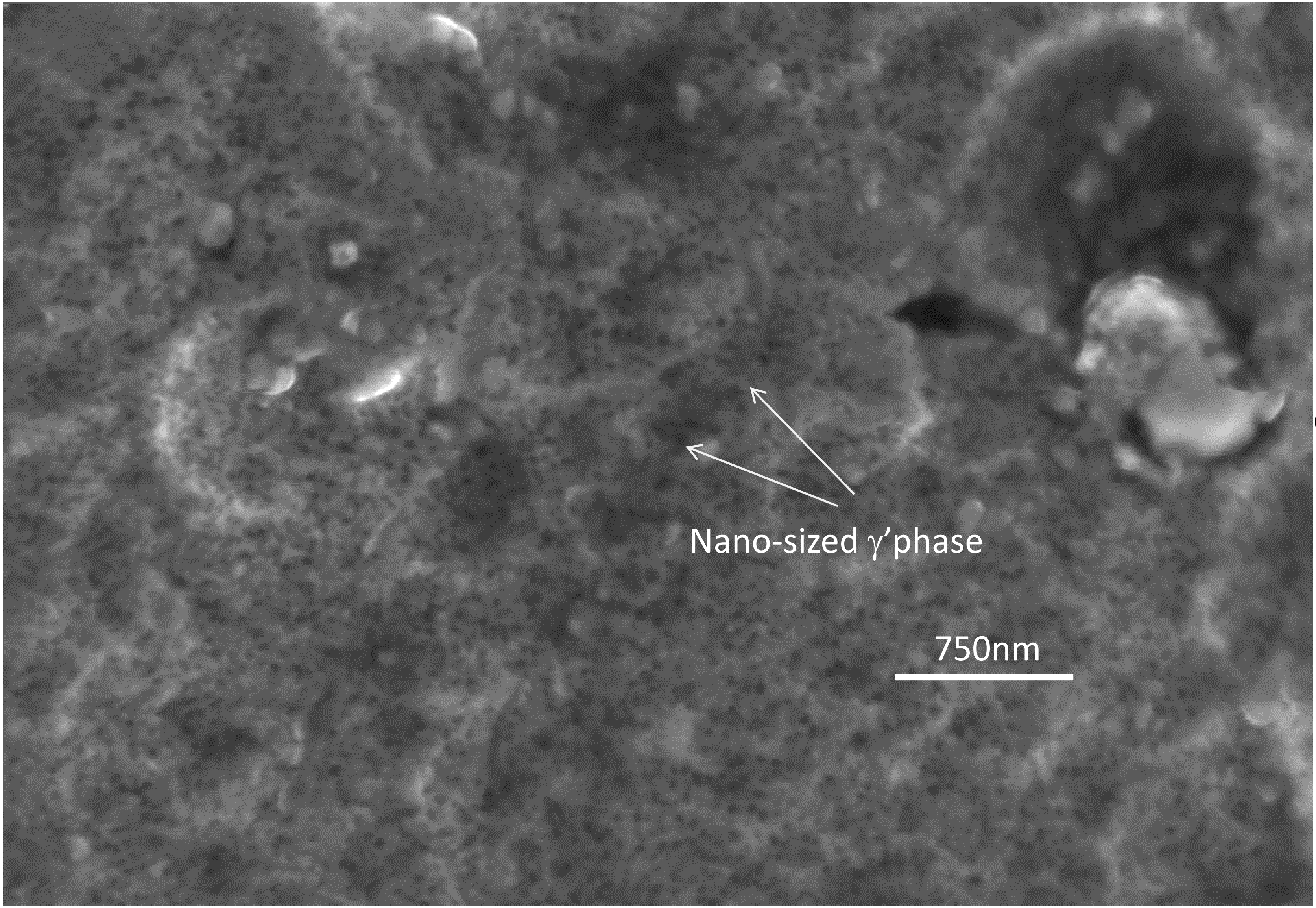

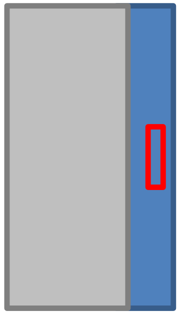

Nano-sized γ'phase preserved at ODS costing after 2200 cycles

Siemens Laser Cladding ODS

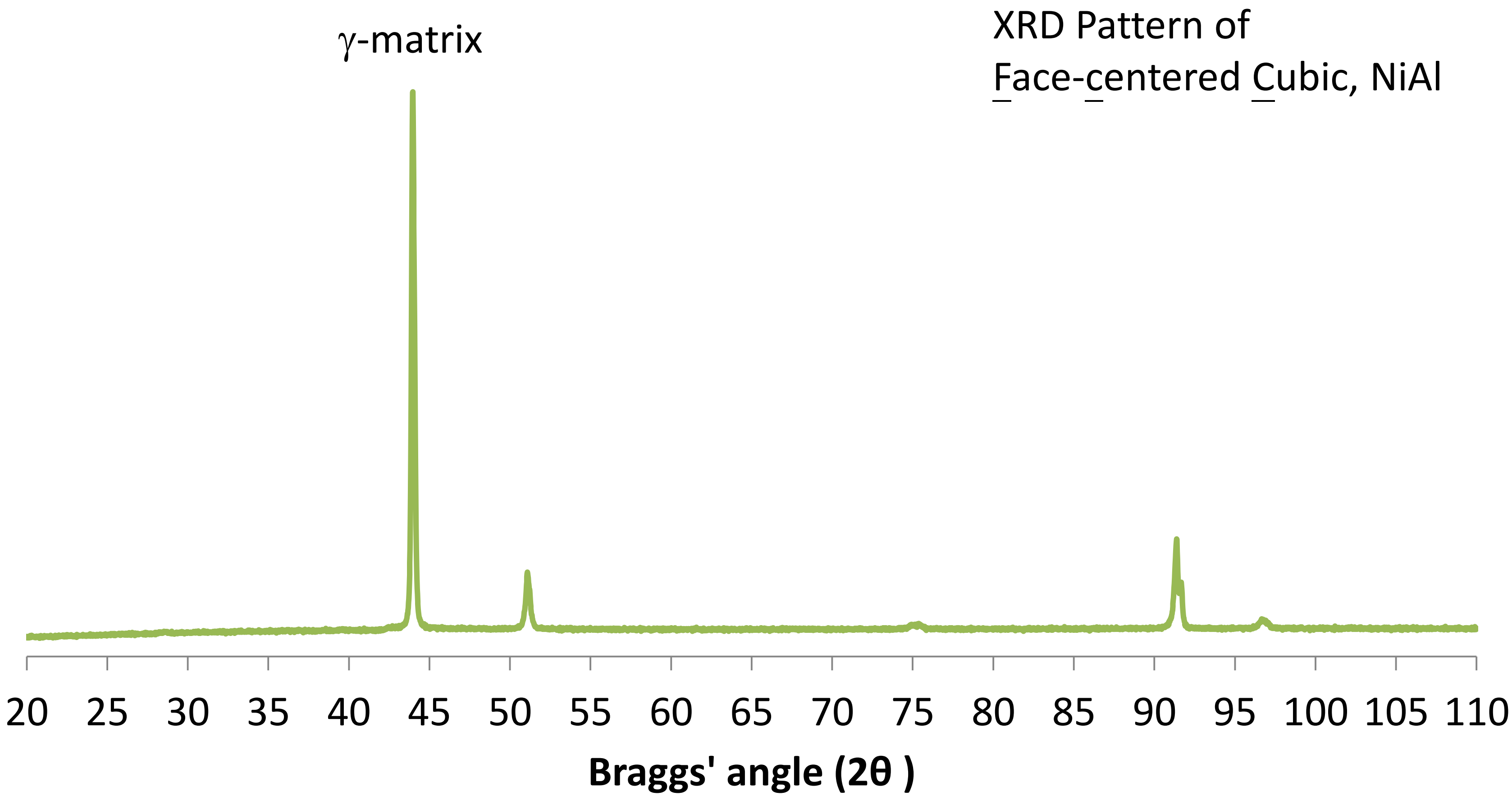

LC ODS Coating

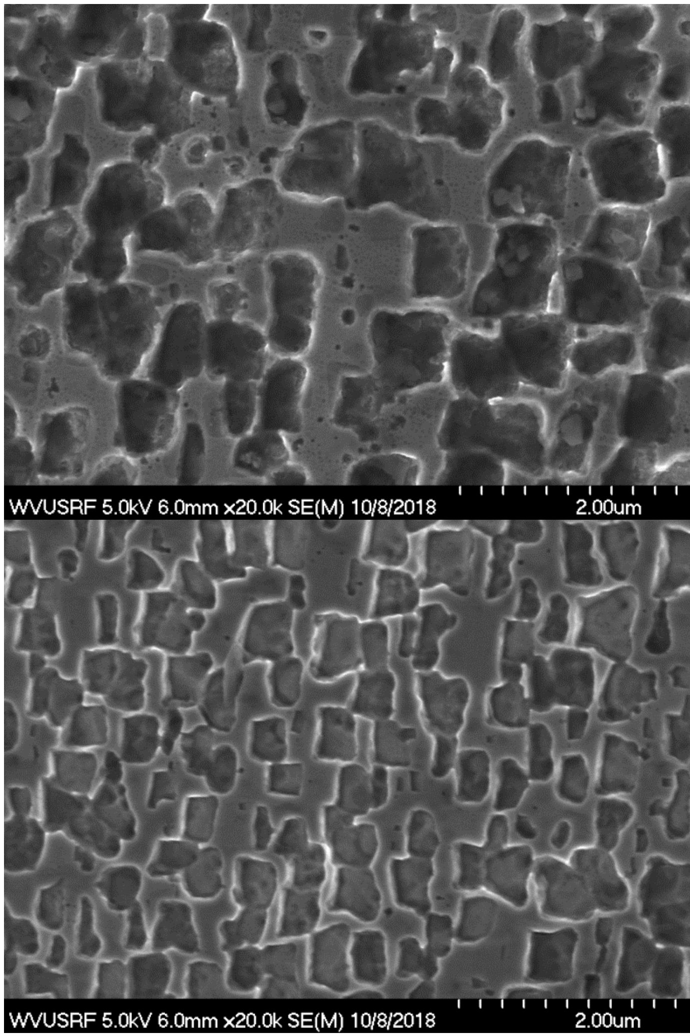

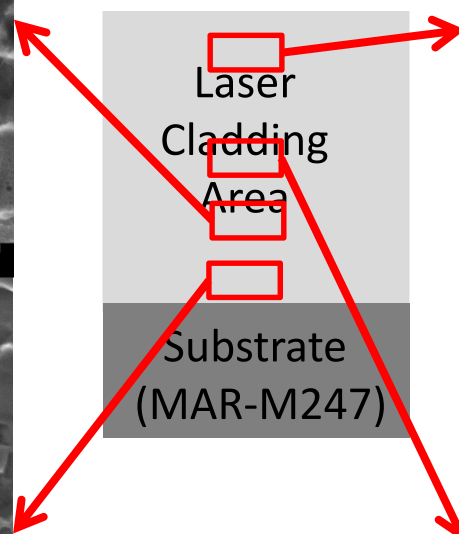

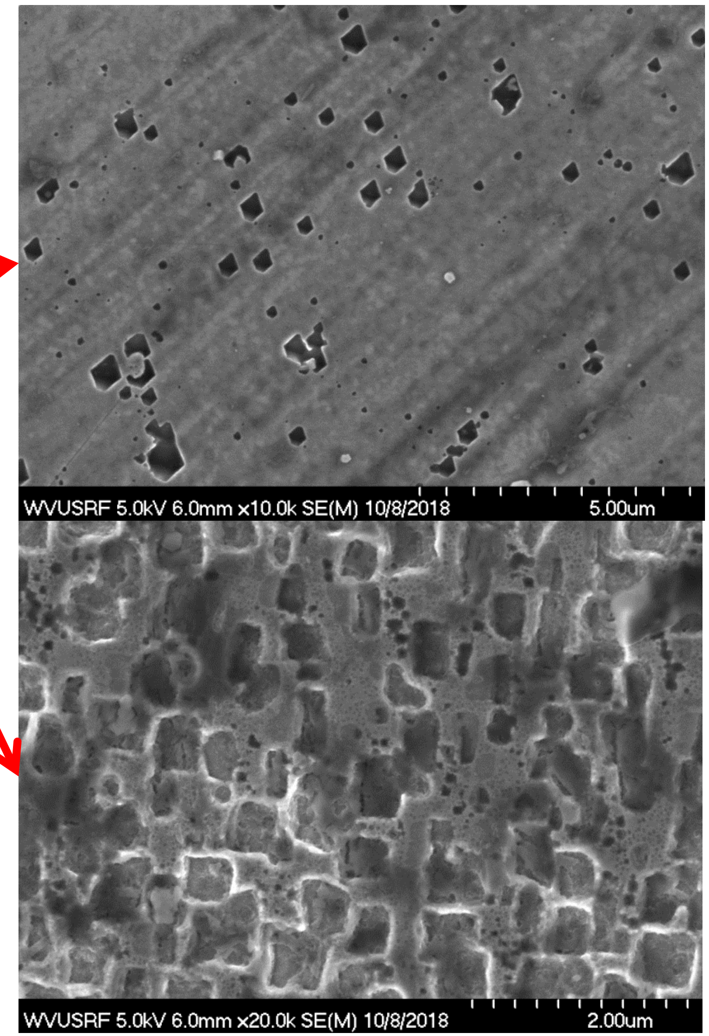

γ'phase variation throughout the layers

Summary for Powder Fabrication and ODS Sample Testing

- ***Development of MCB + BM and MCB-only ODS powder for AM-assisted or LC-processed ODS structural coating for high temperature materials research.***
- ***Long-term isothermal and cyclic thermo-loading tests of AM-assisted ODS coatings and cooling channels were conducted. Test results revealed existence of stable/durable protective alumina oxide layer on coating surface and presence of gamma prime phase in AM-assisted ODS coating.***
- ***AM-Based ODS technologies for protection of turbine hot-section are promising***

Integrated Transpiration & Lattice Cooling

Objective: Design highly efficient and manufacturable integrated transpiration and internal cooling reaching an overall cooling efficiency higher than 0.6.

Approach

- Exploration of transpiration and lattice geometries
  - Transpiration: hole diameter, pitch, porosity, bio-inspired designs
  - Lattice: internal structure, e.g. unit cell geometry and cell matrix arrangement, internal heat transfer surface area
- Integrated design
  - Optimized combined/conjugate transpiration and lattice cooling
  - Porosity affected mechanical strength
  - Effects of AM process
- Experimental and numerical simulation
  - Experimental studies on transpiration (external), lattice (internal) and combined/system system
  - CFD for detailed flow field and vortex structures

Fabrication Methods of Porous Metal

- **Metal foam**: molten metal foamed by gas injection
  - Pros: high porosity, low cost
  - Cons: low strength, little design and process control
- **Metal powder compaction**: metal powders sintering
  - Pros: high porosity, stronger than metal foam
  - Cons: time consuming, difficult in control design and process, non-interconnected voids
- **Metal woven wire matrix**: weaving multi-layer metallic wire meshes followed by sintering
  - Pros: good strength
  - Cons: shape and geometry restriction, costly
- **Direct Metal Laser Sintering**:
  - good geometry control
  - desirable mechanical strength
  - ability to build complex structure
  - reasonable cost – cheaper with time

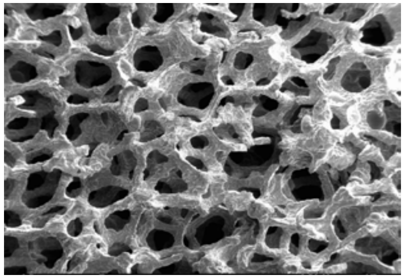

Metal Foam

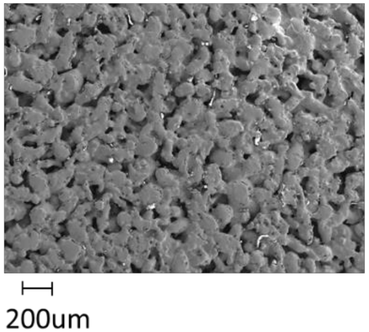

Sintered Powder Pack

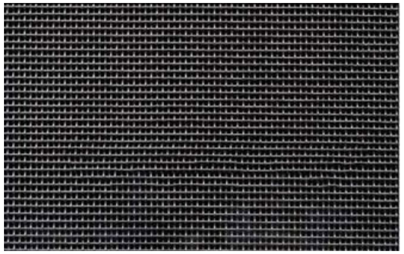

Metal Wire Matrix

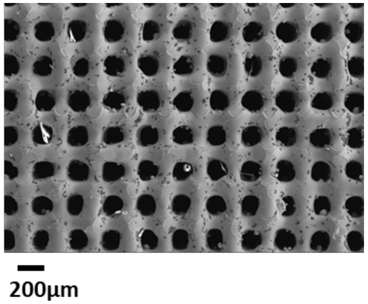

Micro-channels made by DMLS

Direct Metal Laser Sintering (DMLS) Method

Capabilities of Powder Bed DMLS, EOS M290:

- Shape Complexity
- High Resolution
- Functional Complexity
- Feedstock Fluidity And Re-usability

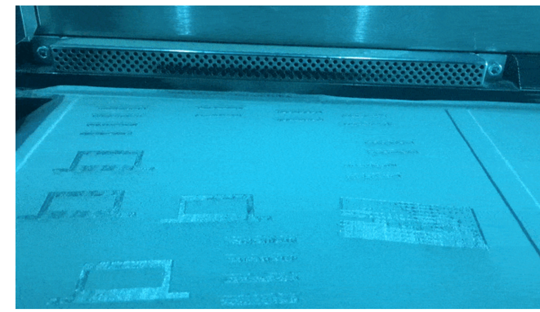

Operating Parameters:

- **Laser Power**: 400W
- **Laser Focal Diameter**: 100μm
- **Scan Speed:** up to 7m/s
- **Printing Material:** Inconel 718

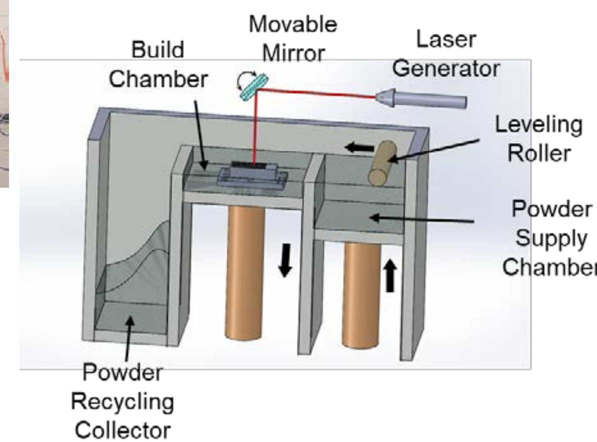

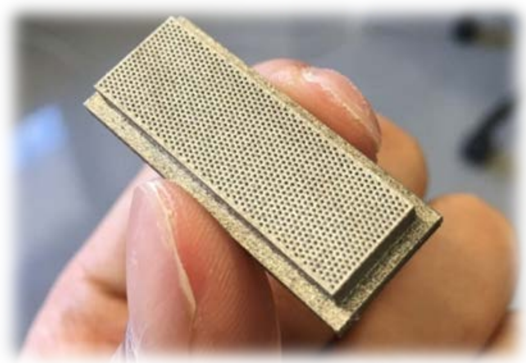

Transpiration & Film Cooling Test Structures

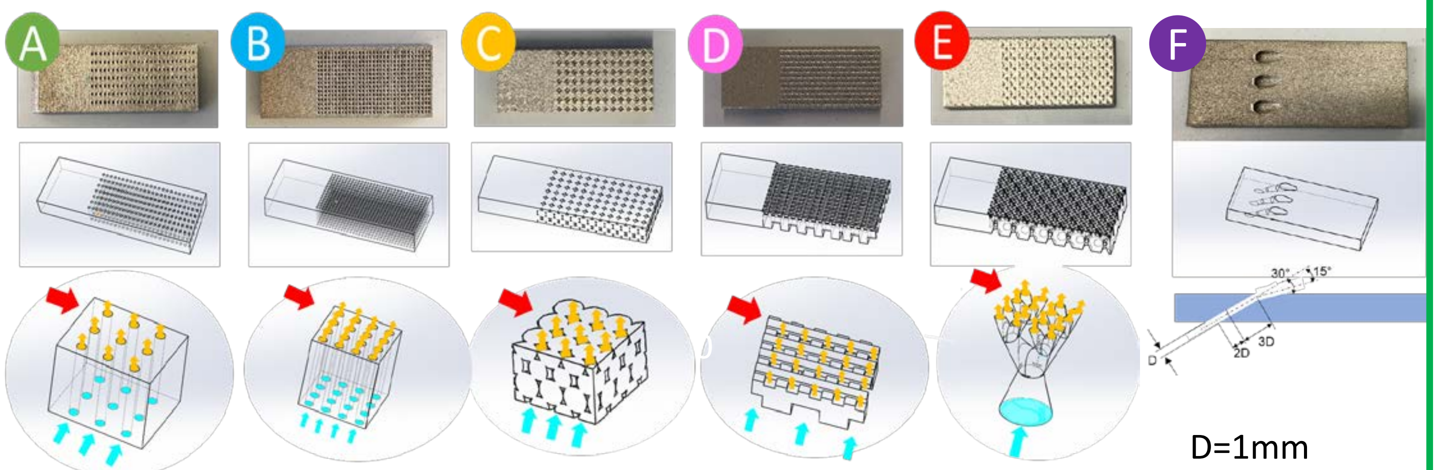

(A) Round Holes with Pitch of 3D (**RH-3D**)

(B) Round Holes with Pitch of 2D (**RH-2D**)

(C) Spheres Packing (**SP**)

(D) Wire Mesh (**WM**)

(E) Blood Vessel Shaped (**BV**)

(F) Laidback Film Cooling (**FC**)

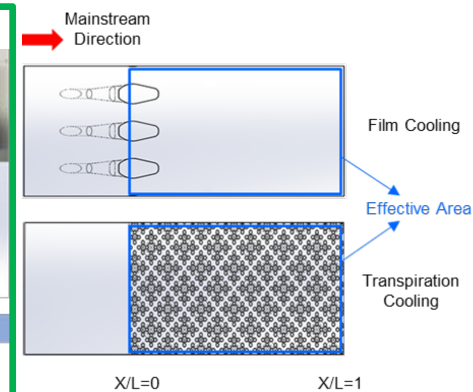

Design Parameters:
Material: In718
Test Plate Size (mm) :
L30×W12×T3.2

Cooling effective area:
L20 ×W12

Injection Ratio: $F = \frac{\rho_c v_c}{\rho_g v_g}$; $v_c = \frac{\dot{m}_c}{\rho_c A_{effective}}$

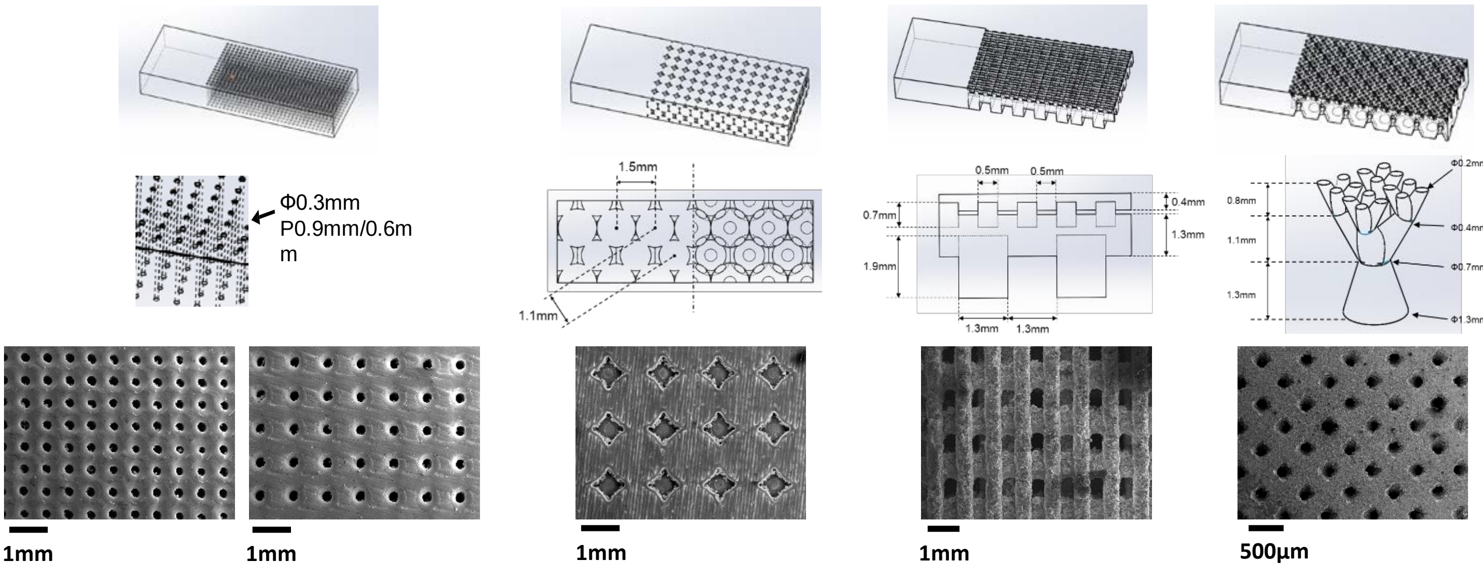

SEM photos show no obvious shape or dimension change of the top surface

Designed Porosity

$$\phi_d = \left(1 - \frac{V_d}{V_{solid}}\right) \times 100\%$$

Porosity determined by weight

$$\phi_m = \left(1 - \frac{M_r}{M_{solid}}\right) \times 100\%$$

Area Ratios: $R_{internal} = \frac{A_{internal}}{A_{effective}}$; $R_{outlet} = \frac{A_{outlet}}{A_{effective}} \times 100\%$

Porosity and Heat Transfer Area Ratios

	Designed Volume(mm^3)	Weight Measured(g)	Designed Porosity	Measured Porosity	Effective Area(mm^2)	Internal Surface Area Ratio	Surface Outlet Area Ratio
Solid	1143	9.24	-	-	-	-	-
Round Holes(P=3D)	1095.8	8.71	4.13%	5.74%	240	2.18	5.15%
Round Holes(P=2D)	1045.7	8.36	8.51%	9.52%	240	6.17	14.58%
Sphere Packing	1020.3	8.32	10.73%	9.96%	240	6.04	13.70%
Wire Mesh Matrix	904.2	7.08	20.89%	23.37%	240	3.26	31.18%
Blood Vessel	989.6	7.81	13.42%	15.48%	240	5.96	18.18%
Film Cooling	1116.5	8.96	2.32%	3.03%	240	0.45	6.65%

Setup for Cooling Effectiveness Measurement

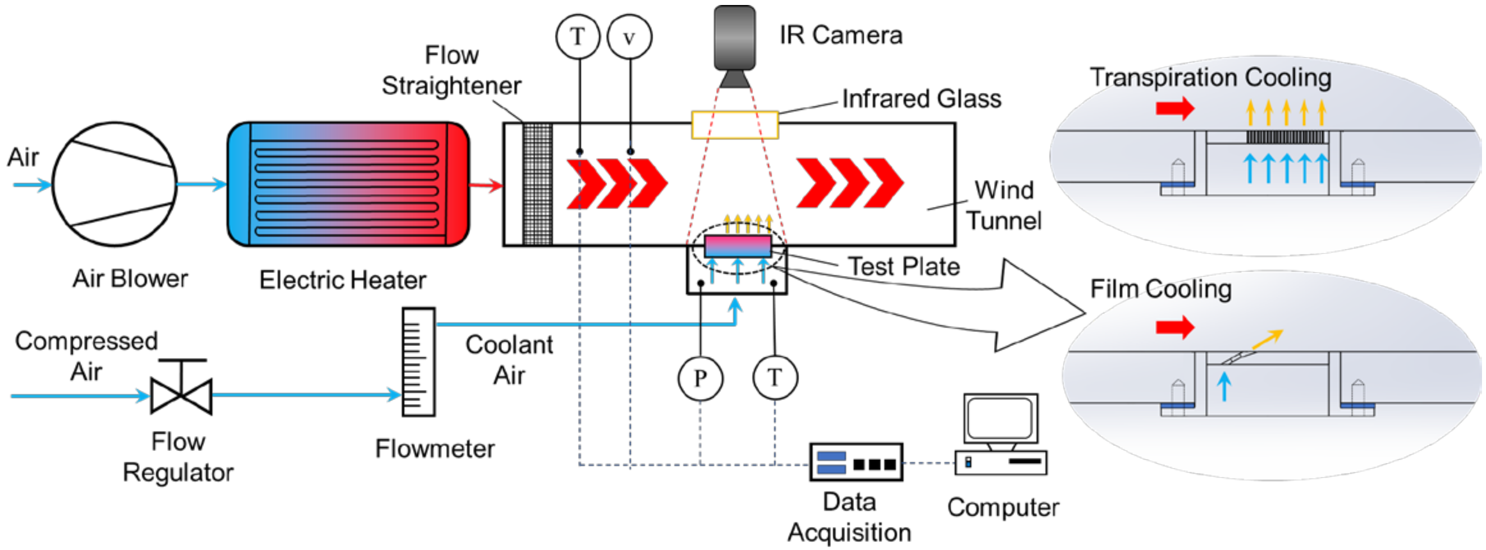

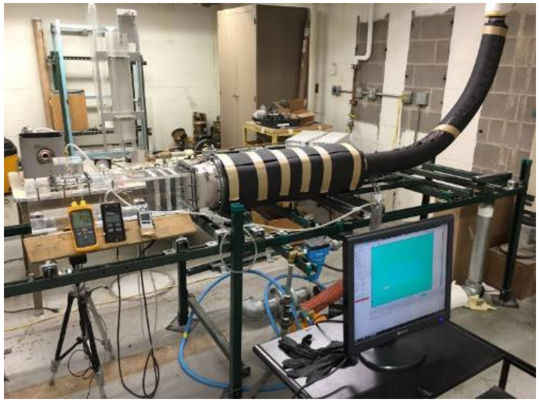

Test Conditions:

1. Injection Ratio: F=1.2%; 2.4%; 3.6%
2. Coolant Temperature: Tc=~21 ℃
3. Mainstream Temperature: T_{gset}=45, 50, 55, 60℃
4. Mainstream Velocity: v_g=11m/s (Re_g=98,000)

Temperature & Film Effectiveness

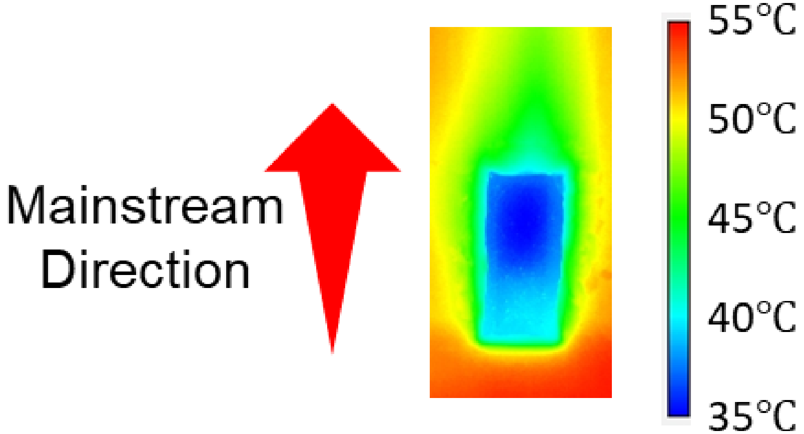

Temperature Distribution

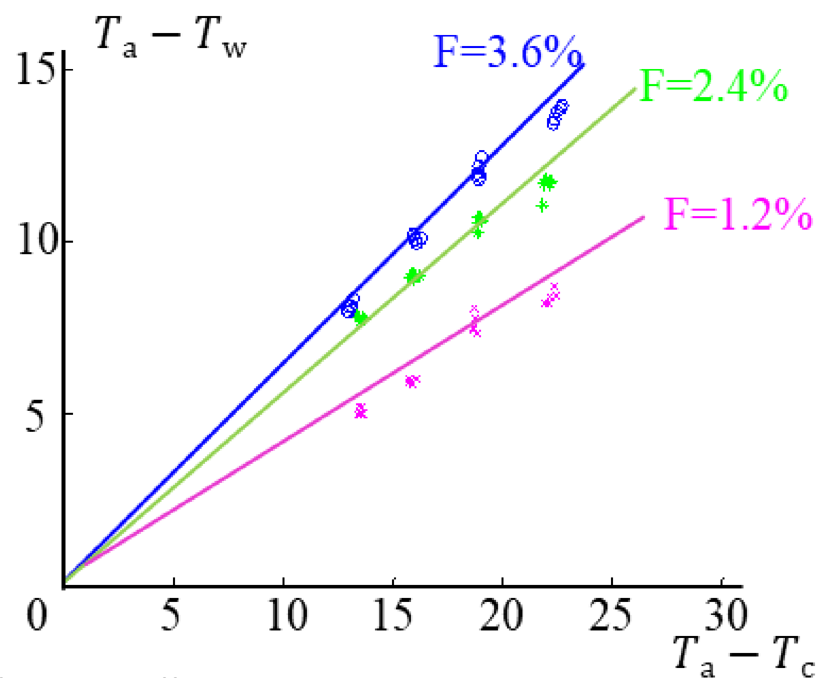

$$\eta = \frac{T_a - T_w}{T_a - T_c}$$

T_a: adiabatic wall temperature
T_w: wall temperature
T_C :coolant temperature

Results – Local Cooling Effectiveness

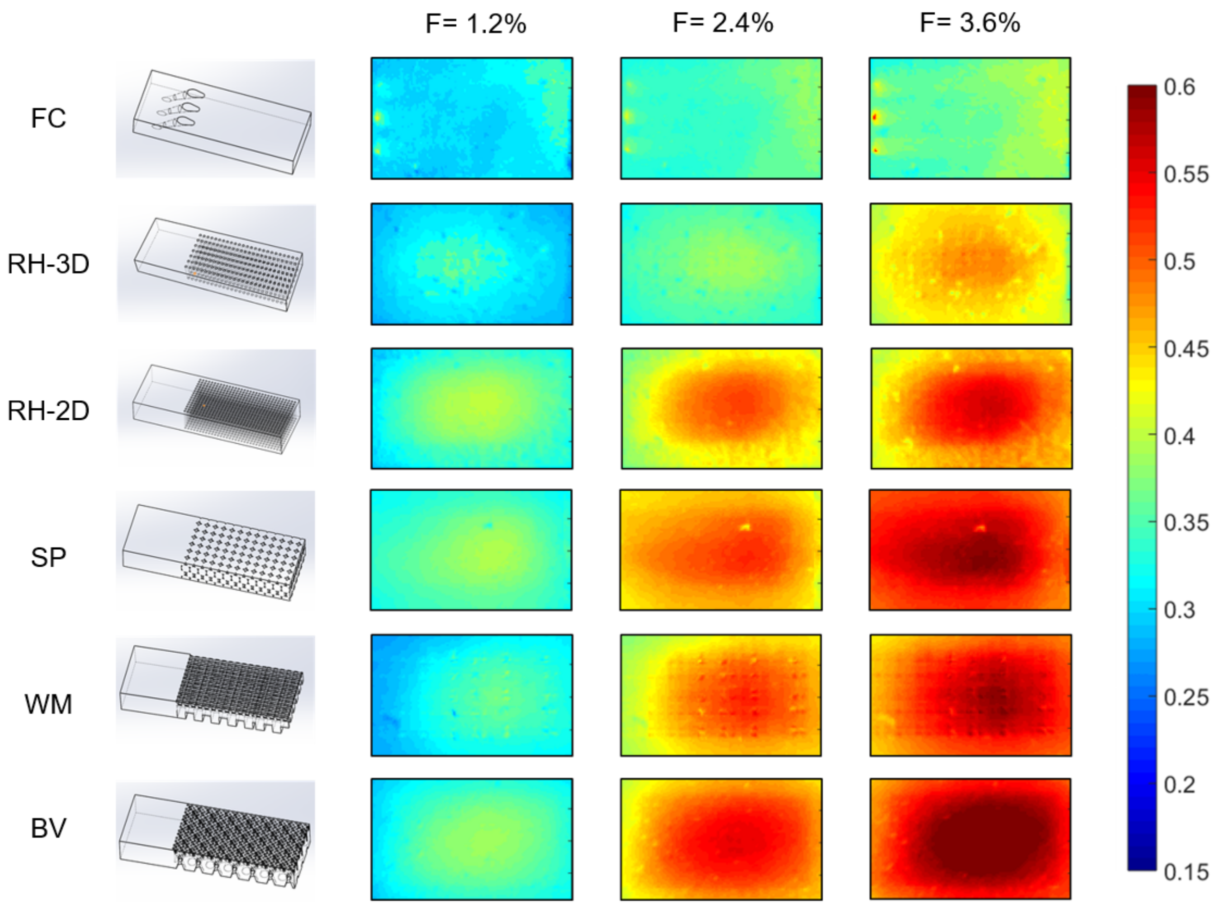

- F=1.2% and 2.4%, except RH-3D (round hole 3D Pitch) , η of all other 4 transpiration structures > η of FC （film cooling case）
- F=3.6%, η of all 5 transpiration structures > FC
- BV (Blood Vessel) and SP (Sphere Packing) are of higher cooling effectiveness η than others
- BV has the highest average cooling effectiveness, η ~ 0.57 for F=3.6%

Streamwise-Resolved, Spanwise-Averaged Cooling Effectiveness

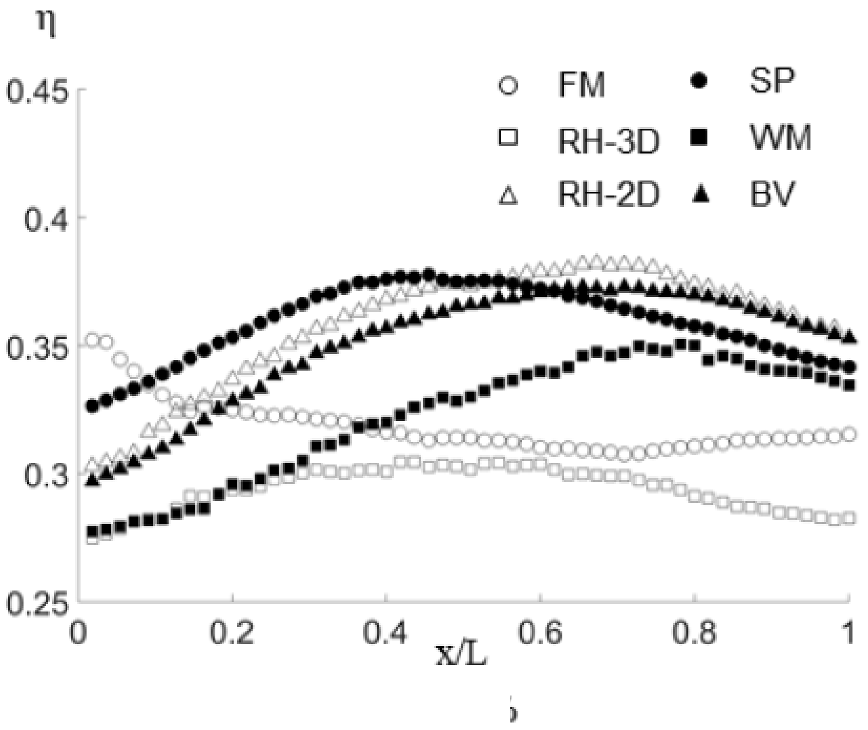

F=1.2%

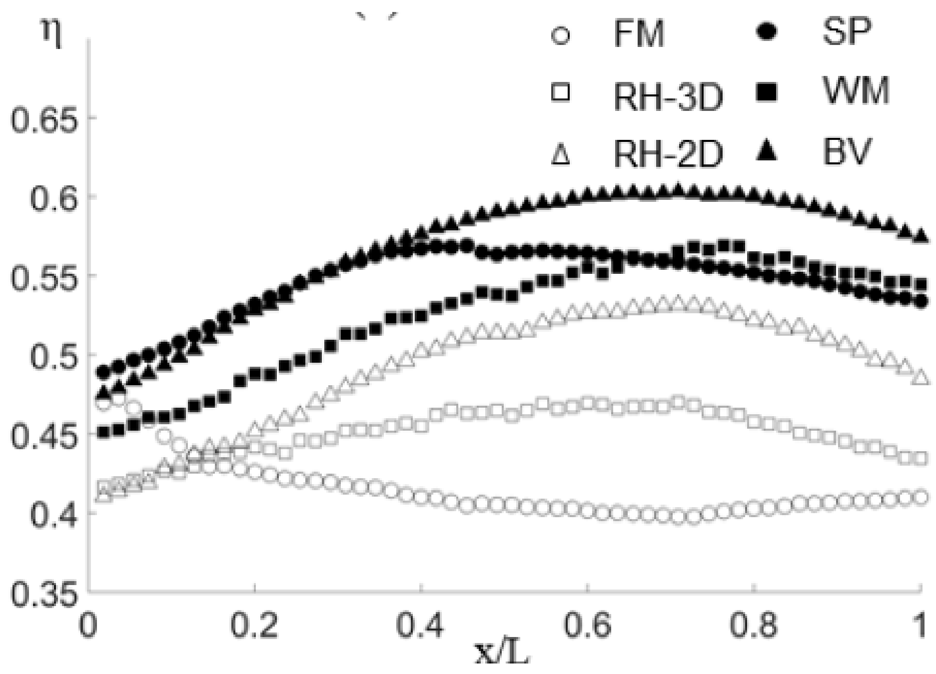

F=3.6%

Effects of Porosity and Internal Surface Area on Cooling Effectiveness

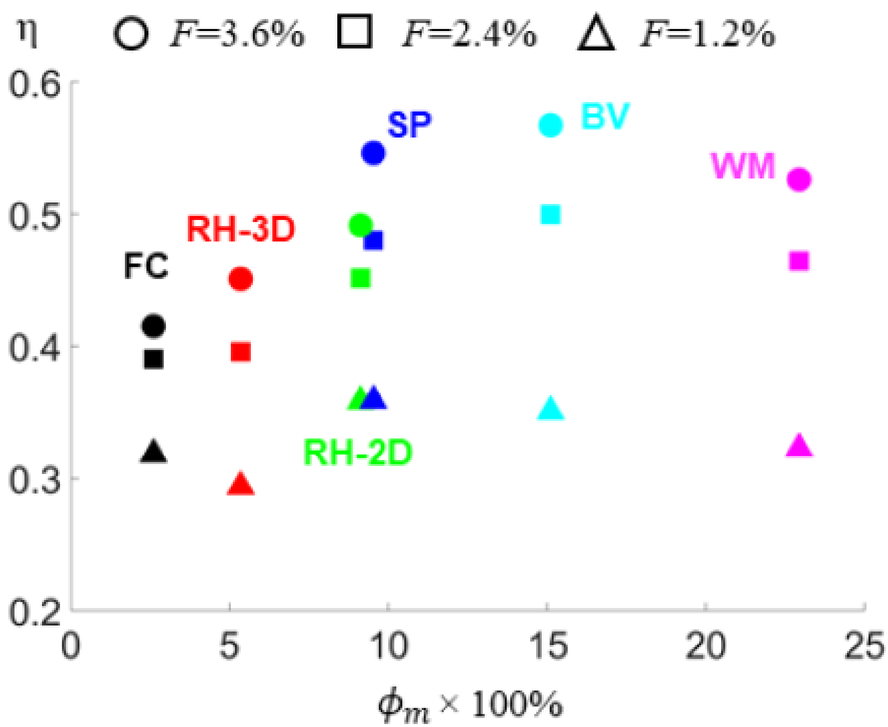

(a) Effectiveness η vs Measured Porosity ϕ

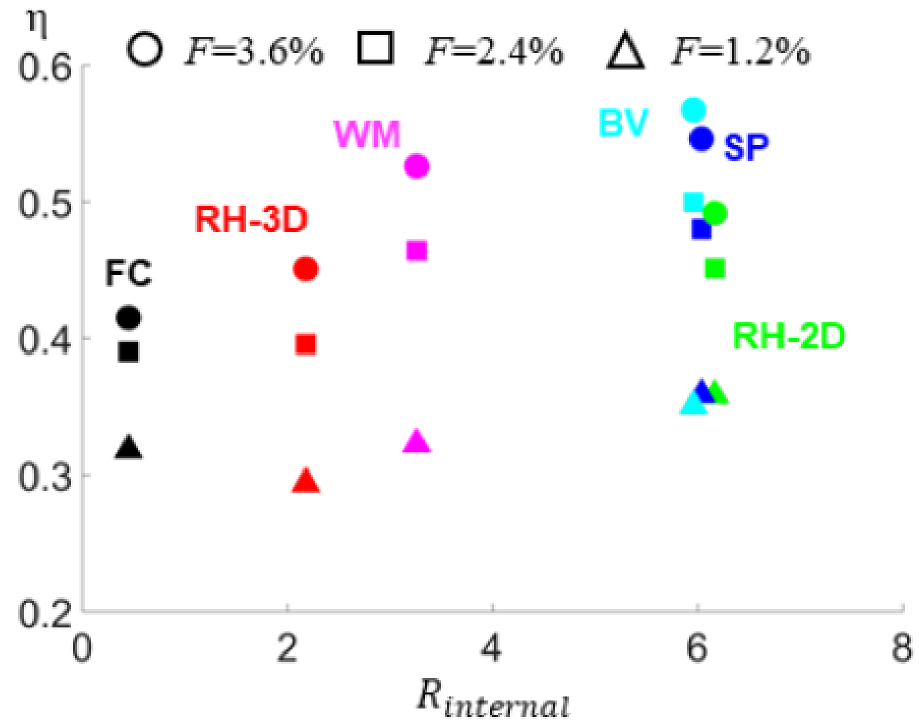

(b) Effectiveness vs Internal Surface Ratio

Tensile Test Results

Tensile Test

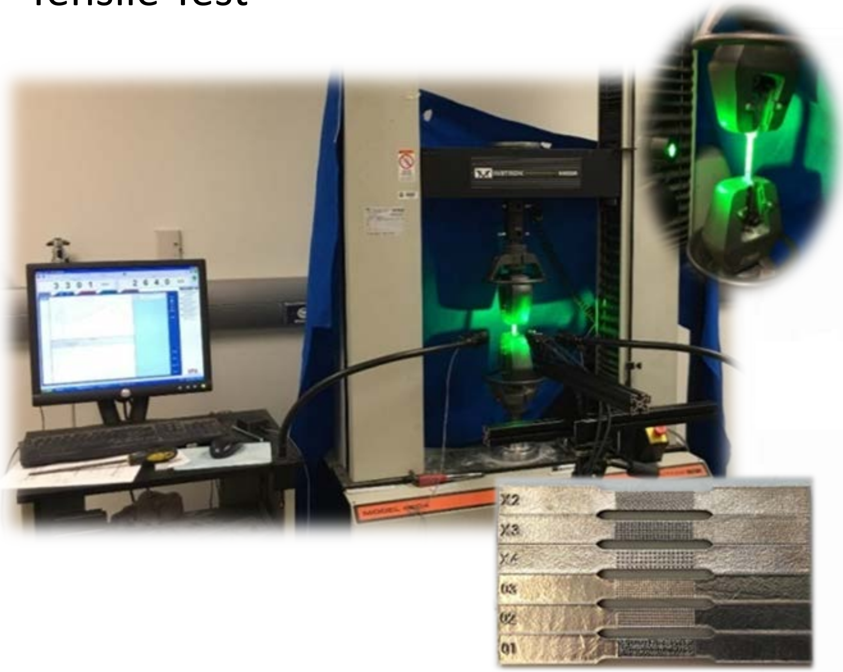

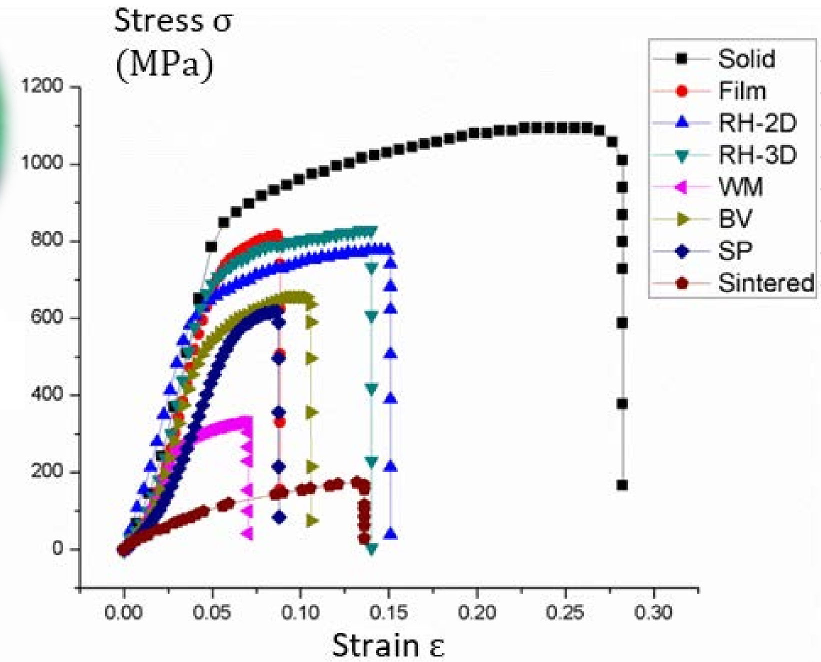

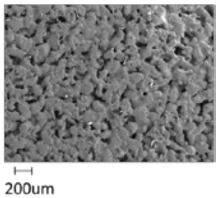

- ➢ Instron 5500R Material Testing System
- ➢ Vic-2D Camera System

- **Maximum Force**: 500kN
- **Test Speed**: 0.5mm/min

All tensile bars made by AM have much higher ultimate tensile strength than the one made by traditional In718 powder sintering(1250C, 6h).

Plot of Cooling Effectiveness vs Tensile Strength

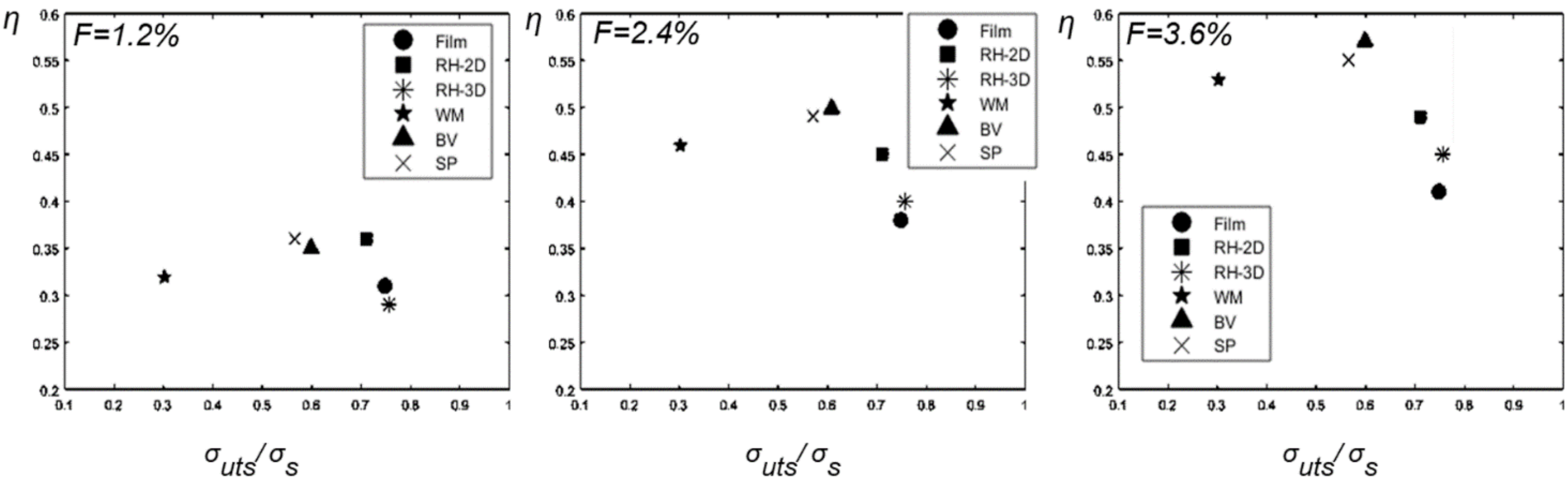

σ_{uts} : Ultimate tensile strength of each coupon

σ_s : Ultimate tensile strength of solid tensile bar

η: Average cooling effectiveness

- **RH-2D, RH-3D, FC**: similar σ_{uts} (**RH-2D**: highest η)
- **BV, WM, SP**: higher η *(when F=2.4%, 3.6%)* but lower σ_{uts}

Task 5: High Temperature Experimental Measurements and Validation

ODS Coated In718 Coupon

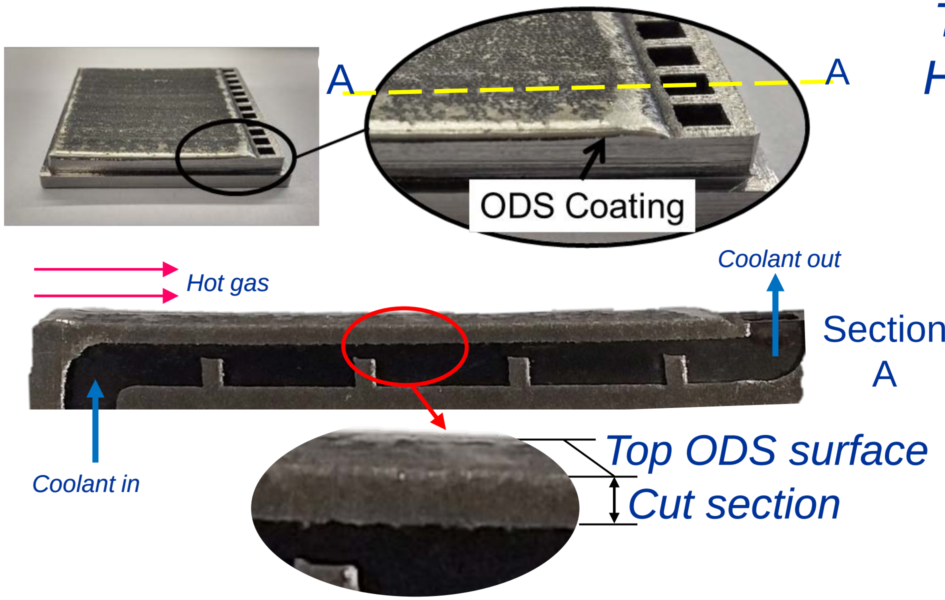

Coating layer intact after exposure to 1100ºC to 1200ºC main gas flow for ~24 hours.

NETL High Temperature, High Pressure Rig

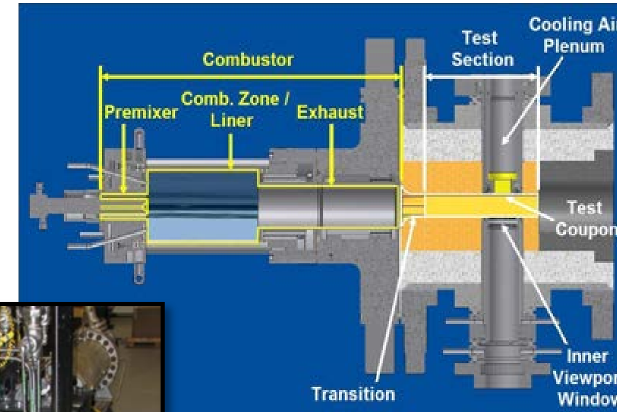

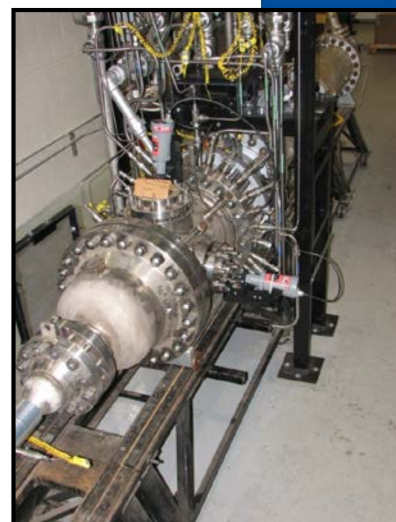

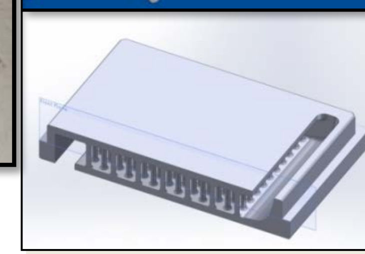

- Conduct HT/P testing at 1100°C for integrated lattice and transpiration cooling
- Further optimization of the lattice structures for enhanced cooling performance
- Address additive manufacturing capabilities for production of parts

Summary from Transpiration Heat Transfer Study

- Five additive-manufactured transpiration cooling structures show higher cooling effectiveness compared to state-of-the-art fan shaped-hole film cooling

- Blood-vessel (BV) structure has the best performance among all five transpiration cooling structures. The highest average cooling effectiveness of BV structure is 0.57 at the injection ratio of 3.6%
- Overall heat removal performance of a transpiration cooling structure is a combined effect of internal convection within porous media and external effused coolant protection
- Current DLMS additive manufacturing process renders significant “off-design” in pore size and geometry. Further studies leading to improved AM built quality are necessary

Thank you!

UTSR Annual Review Meeting, October 30, 2018